

1-1-2006

Monte-Carlo simulation of photoproduction of Omega meson

Parikshit Manoj Junnarkar

Follow this and additional works at: <https://scholarsjunction.msstate.edu/td>

Recommended Citation

Junnarkar, Parikshit Manoj, "Monte-Carlo simulation of photoproduction of Omega meson" (2006).
Theses and Dissertations. 3203.
<https://scholarsjunction.msstate.edu/td/3203>

This Graduate Thesis - Open Access is brought to you for free and open access by the Theses and Dissertations at Scholars Junction. It has been accepted for inclusion in Theses and Dissertations by an authorized administrator of Scholars Junction. For more information, please contact scholcomm@msstate.libanswers.com.

MONTE-CARLO SIMULATION OF PHOTOPRODUCTION OF OMEGA MESON

By

Parikshit M. Junnarkar

A Thesis
Submitted to the Faculty of
Mississippi State University
in Partial Fulfillment of the Requirements
for the Degree of Master of Science
in Physics
in the Department of Physics and Astronomy

Mississippi State, Mississippi

December 2006

MONTE-CARLO SIMULATION OF PHOTOPRODUCTION OF OMEGA MESON

By

Parikshit M. Junnarkar

Approved:

Dr. James Dunne
Associate Professor of Physics and
Astronomy
(Major Professor)

Dr. Wenchao Ma
Professor of Physics and
Astronomy
(Committee Member)

Dr. Jeff Winger
Professor of Physics
and Astronomy
(Committee Member)

Dr. David Monts
Professor of Physics and
Astronomy
and Graduate Coordinator, Department
of Physics and Astronomy

Phillip B. Oldham
Dean of
the College of
Arts and Sciences

Name: Parikshit M. Junnarkar

Date of Degree: December 9, 2006

Institution: Mississippi State University

Major Field: Physics

Major Professor: Dr. James Dunne

Title of Study: MONTE-CARLO SIMULATION OF PHOTOPRODUCTION OF
OMEGA MESON

Pages in Study: 77

Candidate for Degree of Master of Science

The null result of December 2004 Sub-threshold photoproduction of J/ψ experiment has motivated this thesis. This monte-carlo predicts the cross-section for sub-threshold photoproduction process and provides an insight on the cross-section range of these processes.

Additionally calibration runs were performed for Omega and Eta mesons for the verification of correctness of experimental procedure. The results from this experiment are compared with the monte-carlo simulation for the number of omega meson events. This is primarily done as the models for photoproduction of omega meson are well tested. The monte-carlo provides satisfactory results for the photoproduction models and with a crude a spectrometer model predicts the number of events which are off by a factor less than two. A refined model from Jefferson lab will eliminate this discrepancy.

DEDICATION

I dedicate this thesis to my parents. Without their support, I would not have seen this day.

ACKNOWLEDGMENTS

First and foremost, I acknowledge Dr. Dunne for being a great advisor. This thesis would not have been successful without his invaluable guidance and encouragement. I am grateful to him for the financial support and all the unofficial help throughout my program. I appreciate his patience during the research which led to this thesis. I also thank him for allowing me to use his photoproduction code as a tool in this research.

I express my sincere gratitude to my committee members Dr. Wenchao Ma and Dr. Jeff Winger to make themselves available to read this thesis within a very narrow time frame. I express my appreciation for their encouragement.

Special thanks to Mike Okhuysen for being supportive during writing of this thesis.

I am thankful to the Thomas Jefferson National Accelerator Facility (TJNAF) for all the financial, technical and unofficial support during my program. I am also thankful to the Department of Physics and Astronomy at the Mississippi State University for providing me with the opportunity to pursue Master of Science Degree in Physics.

TABLE OF CONTENTS

	Page
DEDICATION	ii
ACKNOWLEDGMENTS	iii
LIST OF TABLES	vi
LIST OF FIGURES	vii
 CHAPTER	
I. INTRODUCTION	1
1.1 From Quarks to Vector-mesons	1
1.2 The Vector Meson Dominance Model	5
1.3 Photoproduction of Vector mesons	6
1.3.1 Rho Photoproduction	7
1.3.2 Omega Photoproduction	8
1.3.3 Phi Photoproduction	8
1.4 Models for J/ψ Photoproduction	10
II. EXPERIMENTAL SETUP	15
2.1 Introduction	15
2.2 Accelerator	15
2.3 Hall C Overview	17
2.4 The Target Vacuum Chamber	18
2.5 High Momentum Spectrometer	18
2.5.1 The HMS Detector Package	19
2.5.2 Scintillator Hodoscopes	21
2.5.3 Drift Chamber	21
2.5.4 Čerenkov Counter	22
2.5.5 Lead Glass Calorimeter	23
2.6 Short Orbit Spectrometer	24
2.6.1 SOS Detector Package	25

CHAPTER	Page
2.6.1.1 Scintillator Hodoscopes	25
2.6.1.2 Drift Chambers	25
2.6.1.3 SOS Čerenkov Counter	26
2.6.1.4 Electromagnetic Calorimeter	26
 III. DATA ANALYSIS AND SIMULATION	 27
3.1 Analysis Software Overview	27
3.2 Omega Analysis	28
3.3 Monte-carlo Simulation	32
3.3.1 Main Event Loop	32
3.3.2 Models for t -dependence	34
3.3.2.1 Diffractive t distribution	35
3.3.2.2 Diffractive and OPE Model for ω	35
3.4 Cross-section for ω Photoproduction	39
3.5 Bremsstrahlung Photons Calculation	43
 IV. RESULTS AND DISCUSSION	 45
4.1 Acceptance Calculations and t -model Results	45
4.1.1 Diffractive Model	45
4.1.2 OPE and Diffractive model	46
4.2 Photon Spectrum	53
4.3 Cross-section Calculations	56
4.4 Number of ω Events	57
4.5 Conclusions and Future Work	58
 REFERENCES	 59
 APPENDIX	
 THE MONTE-CARLO CODE	 60

LIST OF TABLES

TABLE	Page
1.1 Properties of constituents quarks	1
1.2 Lowest Lying multiplets of hadrons in terms of quark model	2
1.3 Reordering of $q\bar{q}$ according to Strangeness S and isospin component I_3	3
2.1 HMS Parameters for Run 52148	20
2.2 SOS Parameters for Run 52148	25

LIST OF FIGURES

FIGURE	Page
1.1 Diffractive cross-section of ρ meson[2]	7
1.2 Diffractive and OPE nature of ω cross-section[2]	9
1.3 Characteristic scales for J/ψ photoproduction near threshold	11
1.4 J/ψ cross-section measurement by Cornell and SLAC	12
2.1 Schematic representation of Linear Accelerator [10]	16
2.2 Schematic representation of Hall-C [11]	17
2.3 Schematic representation of High Momentum Spectromter [7]	19
2.4 Detector package of High Momentum Spectrometer [11]	20
2.5 Schematic representation of Short Orbit Spectrometer [7]	24
2.6 Schematic representation of SOS Detector package [7]	26
3.1 Missing Mass Spectra(ω peak clearly visible near $m_\omega = 0.782$ GeV)	29
3.2 Coincidence timings for ω meson	30
3.3 Background subtracted events for ω	31
3.4 t -dependence for OPE and diffraction from [9]	37
3.5 Presimulation of OPE and Diffractive model for real photons from [9]	38
3.6 Cross-section dependence on Photon Energy [2]	40
3.7 Curve fitted Ballam data	41

FIGURE	Page
3.8 Bremsstrahlung Spectrum [13]	42
3.9 Bremsstrahlung spectrum from MAPLE simulation	42
4.1 Diffractive t distribution	47
4.2 OPE+Diffractive t distribution	48
4.3 Photon Spectrum without Spectrometer cuts for Diffractive model	49
4.4 Photon Spectrum including Spectrometer cuts for Diffractive model	50
4.5 Photon Spectrum without Spectrometer cuts for OPE+Diffractive model	51
4.6 Photon Spectrum including Spectrometer cuts for OPE+Diffractive model	52
4.7 Cross-section results for Diffractive model	54
4.8 Cross-section results for OPE+Diffractive model	55

CHAPTER I

INTRODUCTION

1.1 From Quarks to Vector-mesons

Quarks and Leptons are the fundamental constituents of matter in the standard model of particle physics. The most striking property of quarks is the *confinement*. This property is expected to follow from the theory of strong interactions called Quantum Chromodynamics(QCD) and is also well established experimentally as no free quarks have ever been observed. It is because of this property that quarks are bound inside subatomic particles. Quarks have spin-1/2, hence are fermions and are the building blocks of matter. Table 1.1 summarizes the properties of quarks. The quark model successfully predicts the constituents of all the observed hadrons [8].

Table 1.1

Properties of constituents quarks

Quark	Charge(e)	Spin	I	I_3	S	C	B	Constituent Mass(MeV)
u	$\frac{2}{3}$	$\frac{1}{2}$	$\frac{1}{2}$	$\frac{1}{2}$	0	0	0	330
d	$-\frac{1}{3}$	$\frac{1}{2}$	$\frac{1}{2}$	$-\frac{1}{2}$	0	0	0	336
s	$-\frac{1}{3}$	$\frac{1}{2}$	0	0	-1	0	0	540
c	$\frac{2}{3}$	$\frac{1}{2}$	0	0	0	1	0	1550
b	$-\frac{1}{3}$	$\frac{1}{2}$	0	0	0	0	-1	4800
t	$\frac{2}{3}$	$\frac{1}{2}$	0	0	0	0	0	50000

Table 1.2

Lowest Lying multiplets of hadrons in terms of quark model

Hadron Rest energy (GeV)	Spin-Parity J^π	Type	Members of Multiplets	Number of Members
0.5	0^-	Pseudoscalar mesons	$\pi K \bar{K} \eta \eta'$	9
0.8	1^-	Light Vector-mesons	$\rho K^* \omega \phi$	9
1.1	$\frac{1}{2}^+$	Baryons	$N \Lambda \Sigma \Xi$	8
1.4	$\frac{3}{2}^+$	Baryons	$\Delta \Sigma^* \Xi^* \Omega$	10

Table 1.2 presents a scheme of lowest-lying multiplets of hadrons based on the various flavor combinations of quarks. The rest hadron energy in Table 1.2 is roughly the central energy of the respective multiplet. Hadrons are classified according to their quark content namely baryons with three quarks(qqq) and mesons with a quark and antiquark($q\bar{q}$). We now focus more on the properties of mesons in terms of quarks due its relevance to this thesis.

The intrinsic parity of fermion-antifermion pair being negative and with two spin $\frac{1}{2}$ quarks can form two states with $l = 0$:

$$\begin{array}{lll}
 {}^1S_0 & J^\pi = 0^- & \textit{pseudoscalar mesons} \\
 {}^3S_1 & J^\pi = 1^- & \textit{vector mesons}
 \end{array}$$

To see how the observed mesons (as in Table 1.2) can be understood in terms of their constituent quarks, we consider the relevant masses of quarks from Table 1.1 which are below 1 GeV. Hence, if we consider the three lowest mass quarks u , d and s and their antiparticles in the following combination[8]:

$$u\bar{u} \quad d\bar{u} \quad s\bar{u}$$

$$u\bar{d} \quad d\bar{d} \quad s\bar{d}$$

$$u\bar{s} \quad d\bar{s} \quad s\bar{s}$$

This implies the existence of nine different mesons in agreement with Table 1.2. However, the arrangement is not according to the quantum numbers and hence comparison with experimental observation is not obvious. In Table 1.3, the nine different combinations are arranged according to the strange(S) and isospin(I_3) quantum numbers.

Table 1.3

Reordering of $q\bar{q}$ according to Strangeness S and isospin component I_3

S	$I_3 = -1$	$-\frac{1}{2}$	0	$\frac{1}{2}$	1
1		$d\bar{s}$		$u\bar{s}$	
0	$d\bar{u}$		$u\bar{u}, d\bar{d}, s\bar{s}$		$u\bar{d}$
-1		$s\bar{u}$		$s\bar{d}$	

These can now be compared with nine pseudoscalar and nine vector mesons. For the *pseudoscalar mesons* this scheme gives,

$$\begin{array}{ccccc}
 & & K^0 & & K^+ \\
 \pi^- & & & \pi^0, \eta^0, \eta' & & \pi^+ \\
 & & K^- & & \bar{K}^0 &
 \end{array}$$

and for the *vector mesons*

$$\begin{array}{ccccc}
 & & K^{*0} & & K^{*+} \\
 \rho^- & & & \rho^0, \omega^0, \phi^0 & & \rho^+ \\
 & & K^{*-} & & \bar{K}^{*0} &
 \end{array}$$

In both cases, the assignments for the six states of the *outer ring* are unambiguous. The three states in the center however have the same quantum numbers S and I_3 . Since any linear combination of the states $u\bar{u}$, $d\bar{d}$ and $s\bar{s}$ have the same quantum numbers, it is not possible to identify one quark combination with one meson. Since any linear combination of states $u\bar{u}$, $d\bar{d}$ and $s\bar{s}$ will have the same quantum numbers, we cannot discern one quark combination with one meson uniquely. Since we are concerned only with vector mesons, we now extract the quark content of vector mesons.

In case of rho, since the charged members do not contain any strange quark content, the neutral rho also should not have any strangeness as it forms an isospin triplet with its charged relatives. Now adding up the spin of particle-antiparticle pairs of the states $u\bar{u}$ and $d\bar{d}$, we have

$$\rho^0 = \frac{d\bar{d} - u\bar{u}}{\sqrt{2}} \quad (1.1)$$

In case of ϕ^0 meson, it experimentally observed that in the rest energy spectrum it lies above K^* by 130 MeV and hence must be composed of,

$$\phi^0 = s\bar{s} \quad (1.2)$$

In case of ω , the state function can now be found by setting,

$$\omega^0 = c_1 u\bar{u} + c_2 d\bar{d} + c_3 s\bar{s} \quad (1.3)$$

Now, the state representing ω should be orthogonal to the states representing ρ^0 and ϕ^0 .

From the above considerations of ρ^0 and ϕ^0 , the ω^0 is calculated to be,

$$\omega^0 = \frac{u\bar{u} + d\bar{d}}{\sqrt{2}} \quad (1.4)$$

One immediate observation that we can make here is, since the quark content of ρ and ω are same their masses must be approximately close,

$$m_{\rho^0} \approx m_{\omega^0} \quad (1.5)$$

This observation is indeed found true experimentally.

1.2 The Vector Meson Dominance Model

The Vector Meson Dominance(VMD) model is a non-perturbative, phenomenological model developed in the 1960's to explain photoproduction of light vector mesons. As a result of bulk experimental data[3] during these years, there was a growing awareness that the ability of the photon to transform into a vector mesons might play a broader role than in form factors and decay matrix elements. The VMD provides a physical picture of the photoproduction mechanism and is discussed here to provide the reader with a “physical intuition” of the photoproduction process [3].

The photon interactions with hadrons bear remarkable similarities to purely hadronic interactions. At a very crude level, this can understood if the physical photon $|\gamma\rangle$ were a superposition of two types of states: a bare photon $|\gamma_B\rangle$ and a small-of order $\sqrt{\alpha}$ -hadronic component $\sqrt{\alpha}|h\rangle$ which undergoes conventional hadronic interactions. That is, we expect the important part of the physical photon state to be expressible as

$$|\gamma\rangle \cong \sqrt{Z_3}|\gamma_B\rangle + \sqrt{\alpha}|h\rangle \quad (1.6)$$

where Z_3 introduced to assure the proper normalisation of $|\gamma\rangle$; all states in the above equation have the same 3-momentum k . Invariance considerations dictate that $|h\rangle$ should have

the same symmetry quantum numbers as the photon i.e., $J^{PC} = 1^{--}, Q = B = S = 0$. The copious photoproduction of vector mesons ρ^0, ω and ϕ suggests that they provide very important contributions to $|h\rangle$. The restrictive assertion that these three mesons are the sole hadronic components of the photon, and the bare component $|\gamma\rangle$ cannot interact with the hadrons, is the hypothesis of Vector Meson Dominance(VMD) in its most naive and clear cut form. The less restrictive assumption that all the interactions result from $|h\rangle$, which has more constituents than ρ^0, ω and ϕ is referred to Generalized Vector Dominance(GVD) [3].

1.3 Photoproduction of Vector mesons

This section is devoted to the generalised vector meson photoproduction and a brief overview of dominant mechanisms thereof. The high energy photons (in the order of GeV's) in photoproduction experiments are usually produced by colliding a high energy electron beam onto a radiator or they are generated inside the target as in this experiment.

Generalising the basic picture of the photoproduction process $\gamma p \rightarrow V p$, the photon fluctuates into a quark-antiquark $q\bar{q}$ pair, which then interacts with the proton p . This interaction depends on the mechanisms which will be discussed later. After the interaction, the vector meson V with invariant mass m_V is formed in the first approximation by the $q\bar{q}$ pair. In the kinematic region of centre-of-mass energy $W_{\gamma p}$ the time scales involved are the following: the typical lifetime $\tau_{\gamma \rightarrow q\bar{q}}$ of $\gamma \rightarrow q\bar{q}$ fluctuation and the time $\tau_{q\bar{q} \rightarrow V}$ for the

formation of vector meson V are much longer than the duration τ_i of the interaction with the proton,

$$\tau_{\gamma \rightarrow q\bar{q}} \gg \tau_i, \quad \tau_{q\bar{q} \rightarrow V} \gg \tau_i \quad (1.7)$$

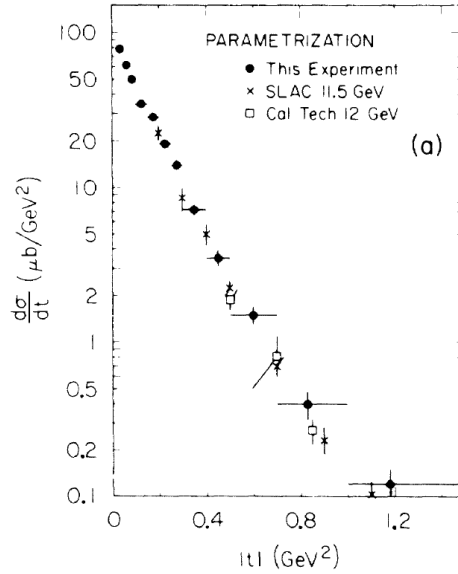


Figure 1.1

Diffractive cross-section of ρ meson[2]

1.3.1 Rho Photoproduction

The rho meson is an unstable particle whose mass and width are roughly 770 MeV and 155 MeV respectively. Its quantum numbers $I^G(J^P)C$ are $1^+(1^-)^-$ and its dominant decay mode is two charged pions [3]. It has been found experimentally that rho photoproduction has characteristics of a diffractive process- i.e., a sharply forward-peaked differential cross section varying slowly in magnitude with photon energy. This is clearly reflected in

the Figure 1.1[2] above. Such behaviour is accounted for in the VMD model by a direct $\gamma \rightarrow \rho^0$ coupling.

1.3.2 Omega Photoproduction

The omega meson is an unstable particle with a mass of (782.7 ± 0.8) MeV and width of (10.0 ± 0.4) MeV. Its quantum numbers $I^G(J^P)C$ are $0^-(1^-)^-$ and its dominant decay modes are $\pi^+\pi^-\pi^0$ ($90.0 \pm 0.6\%$), $\pi^0\gamma$ ($8.7 \pm 0.5\%$) and $\pi^+\pi^-$ ($1.3 \pm 0.3\%$) [3]. Since omega has much a larger width for $\pi^0\gamma$ decay mode than ρ meson, one-pion exchange plays a larger role in omega photoproduction, and at low energies dominates the photoproduction cross-section. In reality the cross-section is sum of diffractive and OPE effect as evidenced in the Figure 1.2 below[2].

Irrespective of the prediction of the OPE effect due to dominant $\pi^0\gamma$ decay mode, the evidence of a large forward peak in differential cross-section in t is a manifestation of the single particle exchange mechanism at work at low t . The one-pion exchange model is specific case of single particle exchange mechanism which was formulated to distinguish between meson exchanges and baryon exchanges which led to forward and backward peaks respectively [12].

1.3.3 Phi Photoproduction

The ϕ meson is an unstable particle with a mass of (1019.7 ± 0.3) MeV and a width of (4.1 ± 0.2) MeV. Its quantum numbers $I^G(J^P)C$ are $0^-(1^-)^-$ and its dominant decay modes

are K^+K^- (46.6 ± 2.3)%, K_LK_S (35.0 ± 2.0)%, $\pi^+\pi^-\pi^0$ (16.4 ± 1.5)%, $\eta\gamma$ (2.0 ± 0.4)% and $\pi^0\gamma$ (0.14 ± 0.05)% [3].

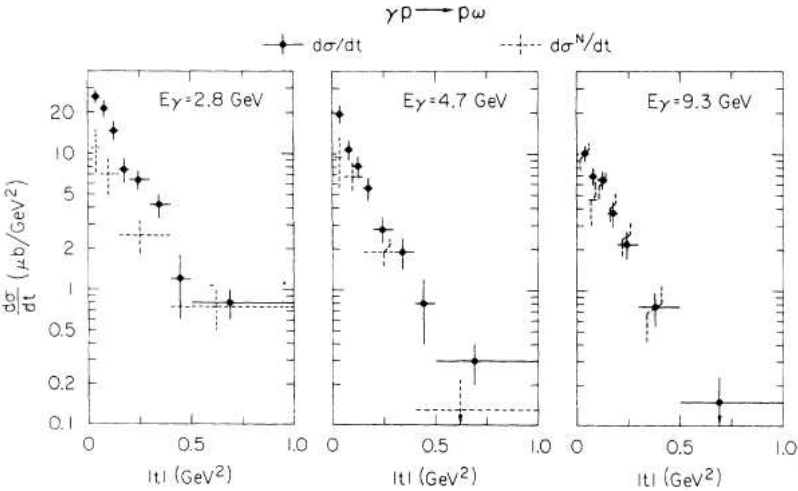


Figure 1.2

Diffraction and OPE nature of ω cross-section[2]

The ϕ meson is interesting from a number of standpoints. In addition to its being one of the three major vector mesons, the ϕp scattering proceeds through Pomeron exchange. This is a consequence of the fact that ϕ is made up of strange-antistrange $s\bar{s}$ which are barred from resonance reactions with nonstrange mesons hadrons. Thus, on the diagonal VMD, one would expect ϕ photoproduction to be due dominantly to Pomeron exchange and hence provides an excellent information concerning Pomerons [3]. The Pomeron is a coherent color-singlet object, built from gluons. It is the object which is exchanged by any pair of hadrons that scatter at high energy and large impact parameter.

1.4 Models for J/ψ Photoproduction

The J/ψ is the first excited state of the bound charm-anticharm quark($c\bar{c}$) with a mass of (3096.87 ± 0.04) MeV and a width of (87.0 ± 5.0) keV. Its quantum numbers $I^G(J^P)C$ are $0^-(1^-)^-$ and its dominant decay modes are to hadrons($87.7 \pm 0.5\%$), e^+e^- ($5.93 \pm 0.10\%$), $\mu^+\mu^-$ ($5.88 \pm 0.10\%$) [5].

In case of photoproduction of J/ψ , the interaction mechanism of J/ψ is not understood to date. The threshold energy in the the center of mass frame for the reaction $\gamma p \rightarrow J/\psi p$ is given by,

$$\sqrt{s} = (m_p + M_{J/\psi}) = 4.034 \text{ GeV} \quad (1.8)$$

The incident photon energy, corresponding to $\sqrt{s} = 4.034$ GeV is,

$$E_\gamma = 8.2 \text{ GeV} \quad (1.9)$$

The maximum available photon energy at the Jefferson Lab is 5.7 GeV, hence to photoproduce the J/ψ the target itself must provide the necessary $P_p > 350$ MeV in the form of Fermi energy. This process is different in this sense as compared to all the photoproduction mechanisms above. Physically this means that the target nucleon momentum must point antiparallel to the incident beam(with the correct energy).

The exact reaction physics of the above process is absent, but there are some specific requirements that are needed to be satisfied for the above process to occur which will broaden our understanding of behaviour of nucleons at short range. Figure 1.3 shows characteristic scales for J/ψ photoproduction near threshold. In this model [4], the photon

fluctuates into a $c\bar{c}$ over longitudinal length, $l_c \approx 2E_\gamma^{lab}/4m_c^2 = 0.36$ fm and interacts with the target proton through gluon exchanges. All the target partons have to transfer their energy to the charm quarks within their proper creation time $1/m_c$ and must be within the transverse distance from $c\bar{c}$. The success of this model is believed to provide a new window into multi-quark.

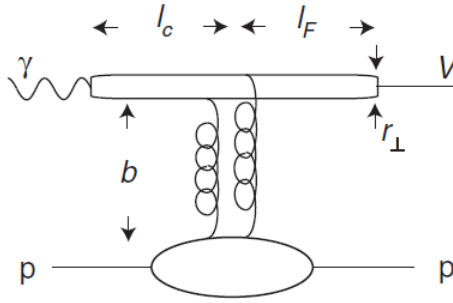


Figure 1.3

Characteristic scales for J/ψ photoproduction near threshold

In case of photoproduction of charm near threshold, since the final nucleon is nearly at rest in the lab frame, the net momentum fraction carried by the spectator partons is $x \sim 0$. The production rate behaves near $x \rightarrow 1$ as $(1 - x)^{2n_s}$ where n_s is the number of spectators. Perturbative QCD predicts three different gluonic components of the photoproduction cross-section[4]:

- The usual one gluon $(1 - x)^4$ distribution for leading twist photon-gluon fusion $\gamma g \rightarrow c\bar{c}$, which leaves two quarks spectators;
- Two correlated gluons emitted from the proton with a net distribution $\frac{(1-x)^2}{R^2\mathcal{M}^4}$ for $\gamma gg \rightarrow c\bar{c}$, leave one quark spectator;
- Three correlated gluons emitted from the proton with a net distribution $\frac{(1-x)^0}{R^4\mathcal{M}^4}$ for $\gamma ggg \rightarrow c\bar{c}$, leaving no quark spectators.

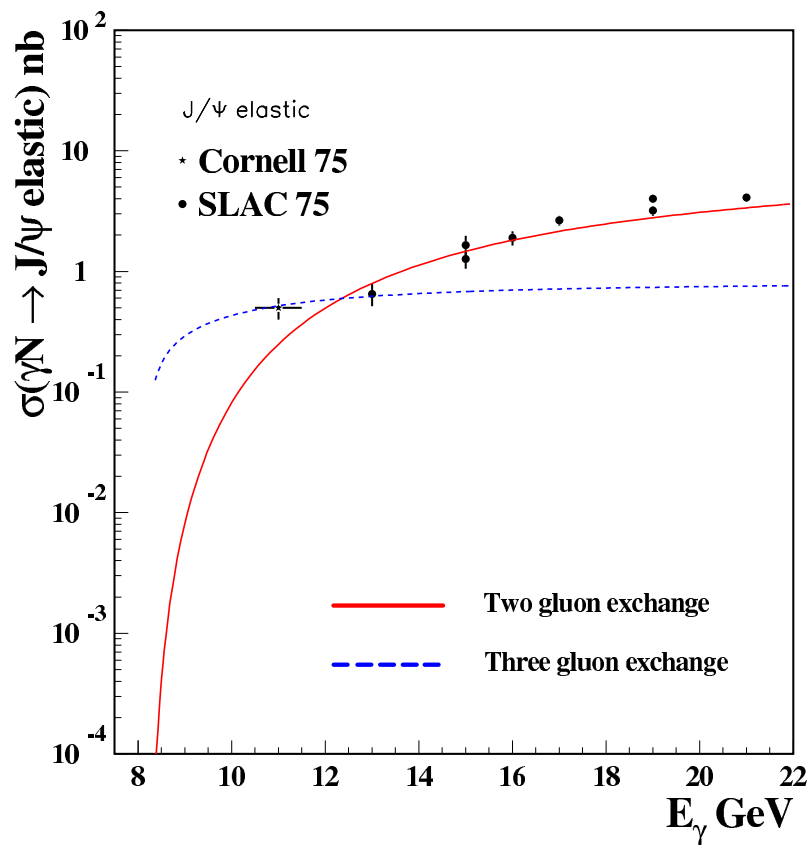


Figure 1.4

J/ψ cross-section measurement by Cornell and SLAC

Here $x \approx (2m\mathcal{M} + \mathcal{M}^2)/(s - m^2)$ and \mathcal{M} is the mass of $c\bar{c}$ pair. For elastic charm production (when the proton target remains bound), it is also necessary to take into the account the recombination of the three valence quarks into the proton via its form factor, as well as the coupling of the photon to the $c\bar{c}$ pair. For the two gluon exchange the cross-section of the $\gamma p \rightarrow J/\psi p$ takes the form[4]:

$$\frac{d\sigma}{dt} = \mathcal{N}_{2g\nu} \frac{(1-x)^2}{R^2 \mathcal{M}^2} F_1\left(\frac{t}{4}\right) (s - m^2)^2 \quad (1.10)$$

while for three gluon exchange it takes the form:

$$\frac{d\sigma}{dt} = \mathcal{N}_{3g\nu} \frac{(1-x)^0}{R^4 \mathcal{M}^4} F_1\left(\frac{t}{9}\right) (s - m^2)^2 \quad (1.11)$$

where \mathcal{N} are the normalization coefficients. $F_1(t)$ is the isoscalar proton form factor and its argument takes into account that the momentum transfer is shared between two or three valence quarks in the proton. These models are used in the monte-carlo simulation in a simplified form[6]: $\frac{d\sigma}{dt} = a f(bt)$:

$f(bt) = e^{bt}$ for the dipole form factor,

$f(bt) = \frac{1}{(1-bt)^3}$ for the 3-gluon exchange model, and

$f(bt) = \frac{(1-x)^2}{(1-bt)^4}$ for the 2-gluon exchange model.

The gluon exchange models are shown with the Cornell and SLAC data as in Figure 1.3 .

While both curves drop off rapidly with photon energies approaching threshold , both the Cornell and SLAC data seem to be flattening out below 12 GeV. It was believed earlier that this was a transition from 2-gluon process to the 3-gluon process near threshold. There are other popular models like the photon-gluon fusion model based on pQCD but these

models fail to match the cornell data by a factor of five and are expected to work at high energy. We present in this thesis analysis of 2-gluon and 3-gluon models.

CHAPTER II

EXPERIMENTAL SETUP

2.1 Introduction

The experiment of Sub-threshold J/ψ photoproduction was conducted at the Hall-C of the Jefferson Lab in November-December 2004. In this experiment, electrons accelerated to the relativistic speeds are collided with a fixed target, which also acts as the radiator for the photon flux via bremsstrahlung. This photon flux further interacts with proton inside the target nucleus to produce an vector meson and proton. Of the several prominent decay modes of the Omega meson, we observed the electron-positron decay mode which has a branching ratio of 7×10^{-5} . These were further detected in coincidence using the two Hall-C spectrometers, the High Momentum Spectrometer (HMS) and the Short Orbit Spectrometer (SOS). The target used was Beryllium with the radiation length of 3%. In this chapter the experimental set up is described.

2.2 Accelerator

The Thomas Jefferson National Accelerator Facility (TJNAF) utilizes two linear accelerators (LINAC), North LINAC and South LINAC, to accelerate the beam over a distance of approximately 2 km and 9 recirculation arcs, East arc and West arc, to bend the beam back in the LINACs. The beam can be recirculated up to a maximum of 5 times and is delivered

to three halls Hall-A, Hall-B and Hall-C with varying energies and currents which is done by splitting the beam at the Beam Switch Yard. At present the accelerator is capable of delivering $200 \mu\text{A}$ and $\sim 6 \text{ GeV}$. The schematic diagram is shown in Figure 2.1

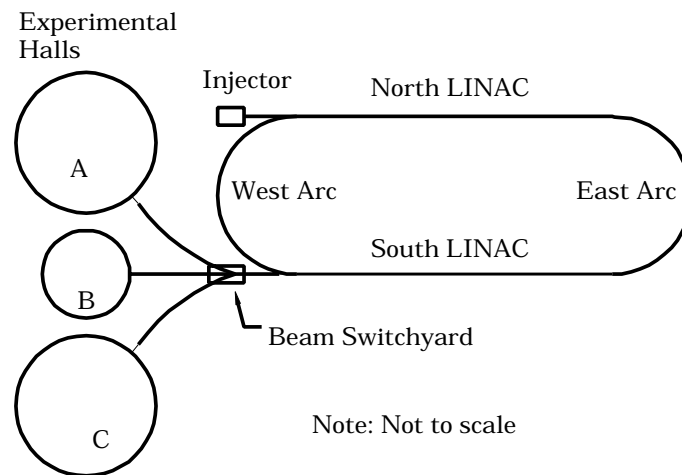


Figure 2.1

Schematic representation of Linear Accelerator [10]

The electron beam is generated in the injector by shining laser light on a Ga-Ar cathode and is injected in the west side of North LINAC at $\sim 45 \text{ MeV}$. In the LINAC, the beam is accelerated in a resonant cavity driven at 1.497 GHz such that an accelerating field is produced which continuously “kicks” electrons in the forward direction. Each LINAC adds upto $500\text{-}600 \text{ MeV}$ in one pass. The beams with different energies is split into different recirculation arcs (namely five) at the north end of east arc. At the re-entry to South LINAC, beams with different energies from the recirculation arcs are focused into single collimated beam and accelerated over the LINAC. According to the energy and current requirement

of the different halls, the beam is either recirculated in the west arc or separated in the Beam Switch yard and fed to the respective hall and collided with a stationary target.

2.3 Hall C Overview

The basic equipments in the Hall C comprise of two spectrometers: High Momentum Spectrometer (HMS) and the Short Orbit Spectrometer (SOS) focused on the target chamber as shown in the schematic Figure 2.2 . This section will describe the Hall C equipment in detail.

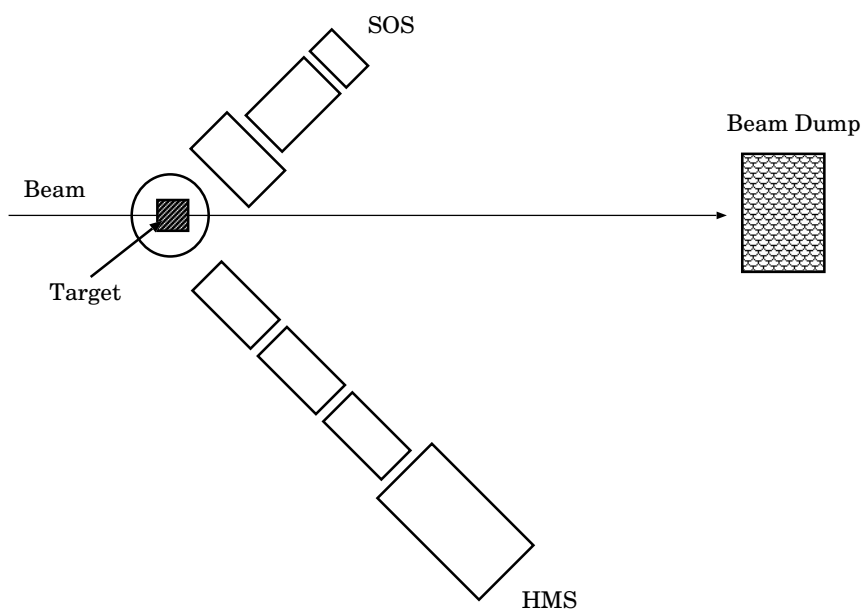


Figure 2.2

Schematic representation of Hall-C [11]

2.4 The Target Vacuum Chamber

The target vacuum chamber is essentially an cylindrical aluminium tank. It was designed to accomodate both solid and cyrogenic target ladder. There are two large openings on the either side of beam entrance and exit. These openings are covered with aluminium windows to minimize the amount of material scattered particles must pass through before entering the spectrometers. Each window on the target chamber is designed to match the range and acceptance of respective spectrometer. Actually, the true opening on the SOS side of the chamber is larger vertically than the acceptance to accomodate the out of plane acceptance of the SOS. The target chamber is also housed with pumping and viewing ports. The lifting mechanism and solid target mechanism are housed on the top cover plate. A solid target of Beryllium with 3% radiation length was used for omega calibration runs. A 4 cm liquid hydrogen target was use for eta calibration runs. The J/ψ production runs use a 6 % radiation length carbon target.

2.5 High Momentum Spectrometer

The High Momentum Spectrometer (HMS) is the largest of the two spectrometers in Hall-C. It is a super-conducting, magnetic spectrometer with a central momentum upto 7.5 GeV/c. In this experiment the HMS was used to detect positively charged leptons in coincidence with negatively charged leptons in the SOS. It comprises of three super-conducting quadrupole magnets and one superconducting dipole magnet in QQD configuration as shown in Figure 2.3. The quadrupole determine the focusing properties of

the spectrometer and hence to a large extent, its acceptance. The dipole magnet bends the focused electrons by an angle of 25° into the detector hut. The HMS was set for the following parameters in this experiment,

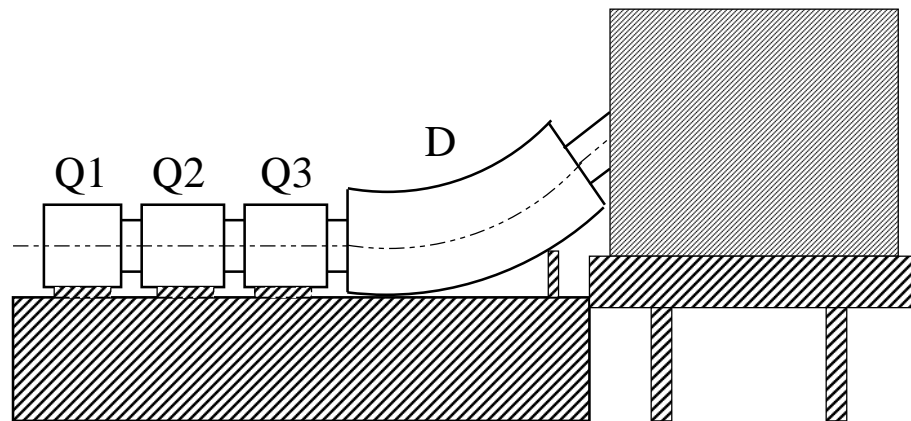


Figure 2.3

Schematic representation of High Momentum Spectrometer [7]

2.5.1 *The HMS Detector Package*

The detector package for High Momentum Spectrometer is shown in Figure 2.4. It consists of two multiwire proportional drift chambers for track reconstruction, a Čerenkov counter for e/π identification, two planes of XY scintillator hodoscopes for triggering and time-of-flight studies, and a lead glass calorimeter for energy measurement and additional e/π discrimination.

Table 2.1

HMS Parameters for Run 52148

HMS Momentum(GeV/c)	2.2	2.2
Q1 Set Current (A)	-254.050	-254.050
Q2 Set Current (A)	201.825	201.825
Q3 Set Current (A)	-98.348	-98.348
Q1 B Field (G)	-3383.9000	-3383.9000
Q2 B Field (G)	4091.9000	4091.9000
Q3B Field (G)	-1976.6000	-1976.6000
D Current Readback	596.310	596.310
B_true	0.5359740	0.5359740
HMS Angle	11.01	13.00

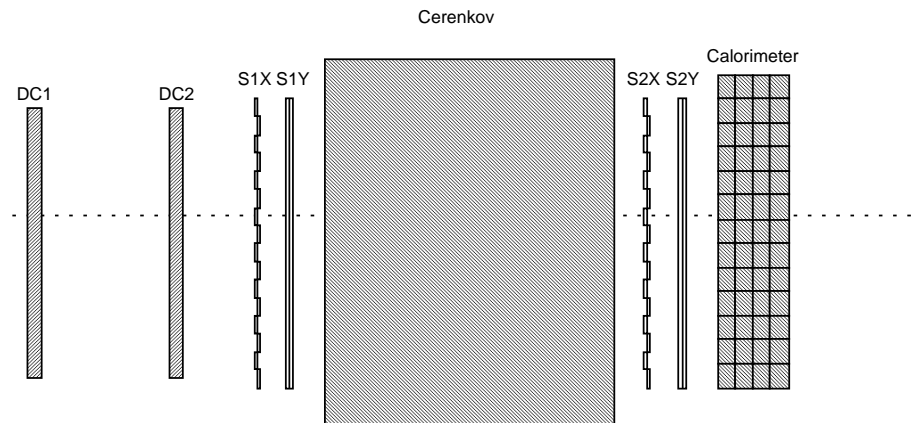


Figure 2.4

Detector package of High Momentum Spectrometer [11]

2.5.2 Scintillator Hodoscopes

A scintillation detector's operation is based on the fact that certain materials emit a small flash of light (scintillation) when struck by a nuclear particle or radiation. When coupled to a conversion and amplifying device such as a photomultiplier tube, these scintillations can be converted into electrical pulses (via the photoelectric effect).

The main purpose of the scintillator hodoscopes in the HMS was to provide a clean trigger. These detectors consisted of four planes. Two of these planes were segmented in X (S1X and S2X as in Fig) and two were segmented in Y (S1Y and S2Y). S1X and S1Y planes were about 2m from S2X and S2Y. Each element was wrapped in aluminium foil for reflection, followed by two layers of Tedlar for external light rejection. The typical trigger was a three out of four coincidence of the scintillator planes.

2.5.3 Drift Chamber

The drift chamber is used to provide position information of the incoming particle in the spectrometer. It consists of six planes arranged in order of X, Y, U, V, X', Y' each 1.4 cm apart as seen by an incoming particle. The fig shows the operation of the drift chamber.

The drift chamber is an ionization detector which consists of basic unit called drift cell. A drift cell is a region of space filled with a gas or gas mixture in which an anode and one or more cathode help establish a stationary electric field. As charged particles pass through the drift cell a certain number of electron-ion pairs are created due to dissociation of gas molecules which are further accelerated in the electric field. During this acceleration, these

charges also collide with other gas molecules and this creates a “drift” towards anode and cathode. The velocity of this collective drift is called drift velocity which depends on the ratio E/p where E is the electric field and p is the gas pressure. The time interval between creation of electron-ion pairs in the cell and their subsequent collection is called “drift time”. By measuring this drift time and knowing the drift velocity one can determine the drift distance, i.e. distance between the sense wire and the trajectory of the initial charged particle passing through cell.

2.5.4 Čerenkov Counter

A charged particle moving in a certain medium at a speed greater than the speed of light emits Čerenkov radiation along a conical wavefront. The angle of emission of θ of the radiation of a given wavelength λ is related to the velocity of the particle relative to the speed of light $\beta = v/c$ and the refractive index n of the medium:

$$\cos \theta = \frac{1}{\beta n} \quad (2.1)$$

The number of Čerenkov photons N_γ emitted per unit length L is given by:

$$\frac{dN_\gamma}{dL} = 2\pi\alpha Z^2 \int_{\lambda_1}^{\lambda_2} \left(1 - \frac{1}{\beta^2 n^2}\right) \frac{d\lambda}{\lambda^2} \quad (2.2)$$

where α is the fine structure constant, Ze is the charge of the particle, and λ_1, λ_2 define the limits of the spectral range of detected radiation.

A threshold Čerenkov counter detects particles that have a velocity sufficient to produce Čerenkov light in the medium, i.e. above a certain velocity threshold. By choosing

the proper index of refraction n , one can set the threshold velocity in such way as to reject the unwanted particles, pions in this case. The appropriate index of refraction to achieve this is in the order of $(10^{-4} \leq (n - 1) \leq 10^{-3})$. Therefore a gas is used as a Čerenkov medium and typically the gas is chosen in such a way so as to maximize the signal for electrons.

The HMS Čerenkov counter used in Hall-C consists of a large cylindrical tank, 150 cm in diameter and 152 cm long. It consists two mirrors which focused light on the photomultiplier tubes. The gas used was C_4F_{10} ($n = 1.00041$). The threshold momentum in this case is 17.9 MeV/c for electrons and 4.9 GeV/c for pions. Hence, it is fully sensitive to electrons. The pressure was set so that it would trigger on muons also.

2.5.5 Lead Glass Calorimeter

The Lead Glass Calorimeter is also called Shower Counter as the measurement is proportional to radiation shower. It served two purposes namely particle identification and energy measurement. The high energy electrons entering the counter interact with the glass and radiate through Bremsstrahlung. These Bremsstrahlung photons further produce electron-positron pairs which inturn radiate more generating a cascade. The high energy electrons from above processes generate Čerenkov light as they are passing through glass which is collected by photomultiplier tubes. Hence, the collected Čerenkov light is proportional to energy of incident of electrons.

The HMS shower counter consists of 52 lead glass blocks. Lead glass is a transparent glass composed of lead dioxide and silicon dioxide. These blocks are stacked in a group of 13 and placed in 4 layers across the incident path. A photomultiplier tube is placed at one end of each block.

2.6 Short Orbit Spectrometer

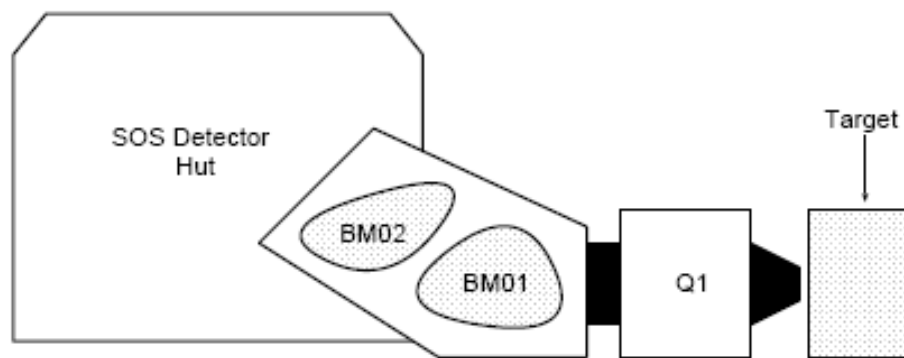


Figure 2.5

Schematic representation of Short Orbit Spectrometer [7]

The Short Orbit Spectrometer (SOS) is magnetic spectrometer with water cooled conventional resistive magnets. The SOS combines a large acceptance, with solid angle and momentum, with a relatively short path length to the focal length. Hence called the Short Orbit Spectrometer. It is primarily designed to detect short lived particles. The maximum central momentum of the SOS is 1.5 GeV/c. It consists of one quadrupole magnet and two dipole magnet in Q, D, -D configuration. The first dipole bends the single charged particles of the central momentum upwards by 33° and the second dipole bends the beam

downwards by 15° , resulting in a 18° through the detectors. The SOS was set with the following parameters in this experiment:

Table 2.2

SOS Parameters for Run 52148

SOS Momentum(GeV/c)	-0.9	-0.9
SOS Angle	25.18	27.83
SOS Quad Momentum	-0.9	-0.9
SOS Dipole 1 Momentum	-0.9	-0.9
SOS Dipole 2 Momentum	-0.9	-0.9

2.6.1 SOS Detector Package

The SOS detector package is similar to that of HMS. It consisted two drift chambers, a Čerenkov counter for particle identification, pair of XY scintillator hodoscopes and a shower counter for energy measurement and additional e/π discrimination.

2.6.1.1 Scintillator Hodoscopes

The SOS hodoscope was similar to HMS hodoscope. It consisted of four layers (two X-planes, SX1 and SX2 and two Y-planes, SY1 and SY2). The SOS scintillators were mounted in aluminium frames, wrapped in one layer of aluminized mylar.

2.6.1.2 Drift Chambers

The SOS drift chamber module consisted of six planes X, X', U, U' . The U and U' were rotated 60° clockwise from X and the v and V' planes are rotated 60° counterclockwise

with X. A schematic view of the drift chamber is shown in the figure. It has three planes of gold-plated tungsten wires of two thickness: 30μ wires at ground potential, and 60μ wires held at negative potential. The gas used in SOS drift chambers was 50-50 mixture of argon and ethane.

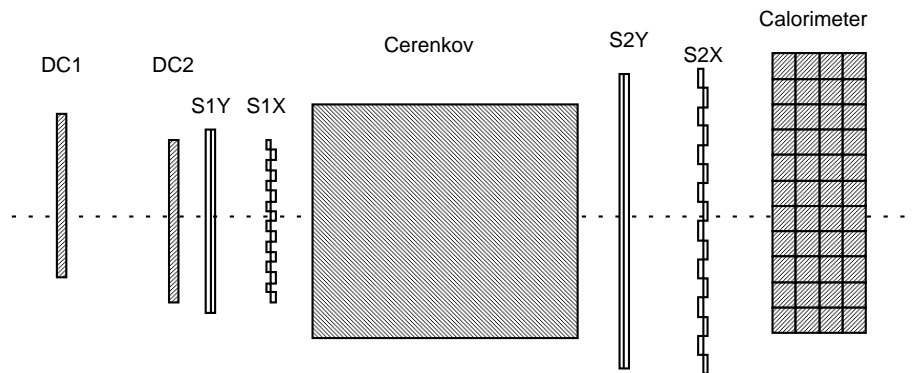


Figure 2.6

Schematic representation of SOS Detector package [7]

2.6.1.3 *SOS Čerenkov Counter*

A new Čerenkov detector was used in the SOS to be able to separate the muons from pions. The tank was pressurized above at 1.8 atm. The detector was modified from the 1.6 GeV SLAC end station Čerenkov detector. The gas used was C_4F_{10} .

2.6.1.4 *Electromagnetic Calorimeter*

The SOS electromagnetic calorimeter consisted of four stacks of TF1 lead glass. Each stack contained seven blocks. The blocks were identical to that HMS.

CHAPTER III

DATA ANALYSIS AND SIMULATION

This chapter provides a description of data analysis and monte-carlo simulation of photoproduction of vector mesons.

3.1 Analysis Software Overview

The experimental data for photoproduction runs of omega was analysed using the Hall-C analysis software(ENGINE). This section serves only an overview of the software functions as a detailed review is beyond the scope of this thesis[1].

The ENGINE is designed as a general purpose analysis software for Hall-C. The code for the software can be easily modified according to the needs of the various experiments that use the standard equipments(i.e. HMS and/or SOS). The raw data acquired from the experiment is recorded to the hard disk drive and backed up to the JLAB StorageTeK robotic library. The data is then retrievable and can be analysed by the replay software. The main tasks of this software will be very briefly reviewed here [11]:

- CODA event decoding - decode the hardware event information and translate into detector arrays .
- HMS and SOS reconstruction - reconstructs trajectories and records particle information for each event.
- Coincidence calculations - calculate the coincidence physics quantities, if both HMS and SOS have a trigger, and store all results.

3.2 Omega Analysis

In this section, the results from the omega runs are presented which will be further compared with the simulation from the monte-carlo. This experiment was set to detect the leptonic decays of vector meson but due to the cleaner sample of e^+e^- decays, this analysis focussed on electrons instead of both electrons and muons. A clear peak for omega was observed which was also evident from coincidence timing settings.

The invariant mass spectrum for omega for the interaction $\gamma p \rightarrow \omega p$ is calculated as follows,

$$M_{\omega}^2 = (P_{e^+} + P_{e^-})^2 \quad (3.1)$$

where, P_{e^+} and P_{e^-} are the 4-momenta of decay leptons as detected in the spectrometers. One can also observe that, as it was mentioned earlier that $m_{\rho^0} \approx m_{\omega^0}$, there two peaks on top of each other, the top one corresponding to ω meson and the bottom one corresponding to ρ meson which is clearly seen in Figure 3.1 The coincidence timings plots as in Figure 3.2 indicate a clear peak for e^+e^- and e^-h^+ coincidence. These observations confirm the particle ID to be omega meson. The calculation of number of ω events is done by background subtraction of Figure 3.1 and is indicated in Figure 3.3

The background separated omega events are fitted with a gaussian whose mean value is exactly the ω mass which is 0.782 GeV with the correct width of 8 MeV. The area under this peak is simply the number of ω events which is calculated using the Physics Analysis Workstation(PAW) software. The result gives 160 events.

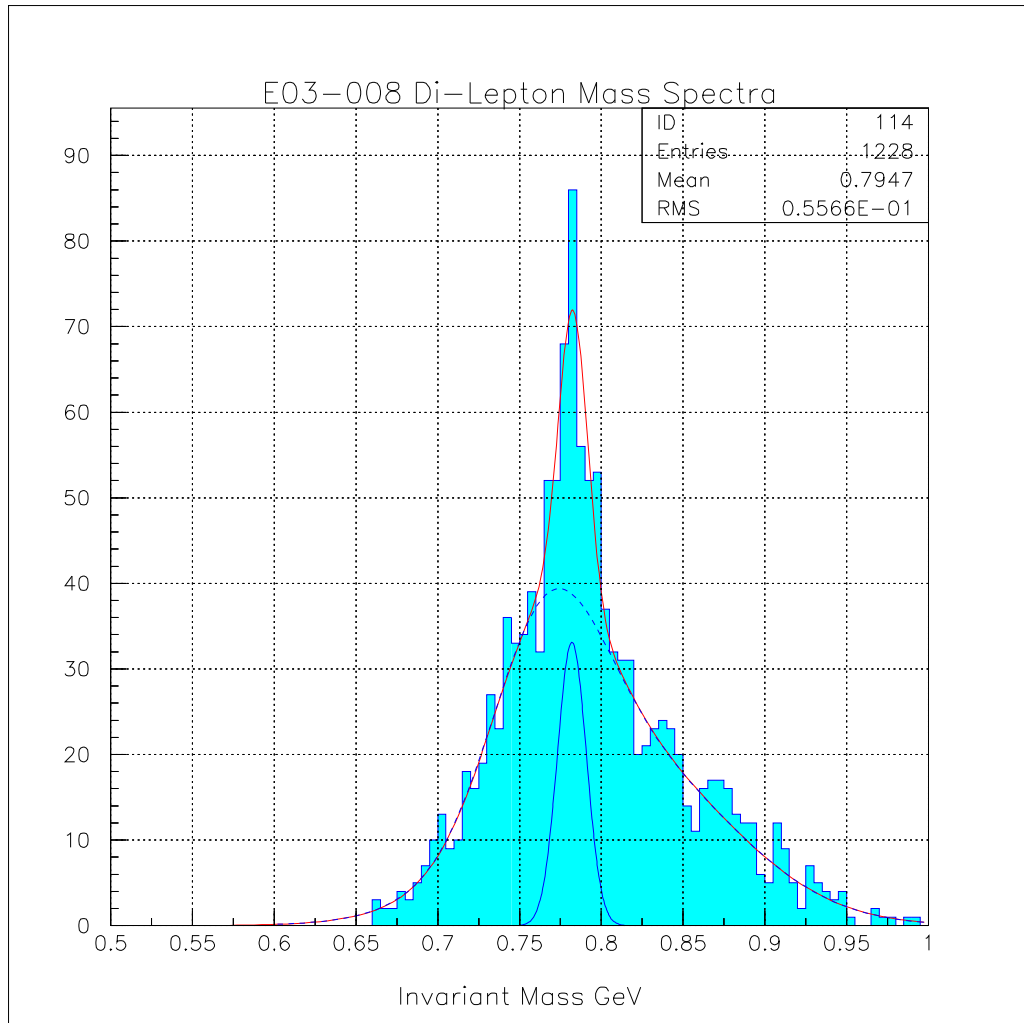


Figure 3.1

Missing Mass Spectra(ω peak clearly visible near $m_\omega = 0.782$ GeV)

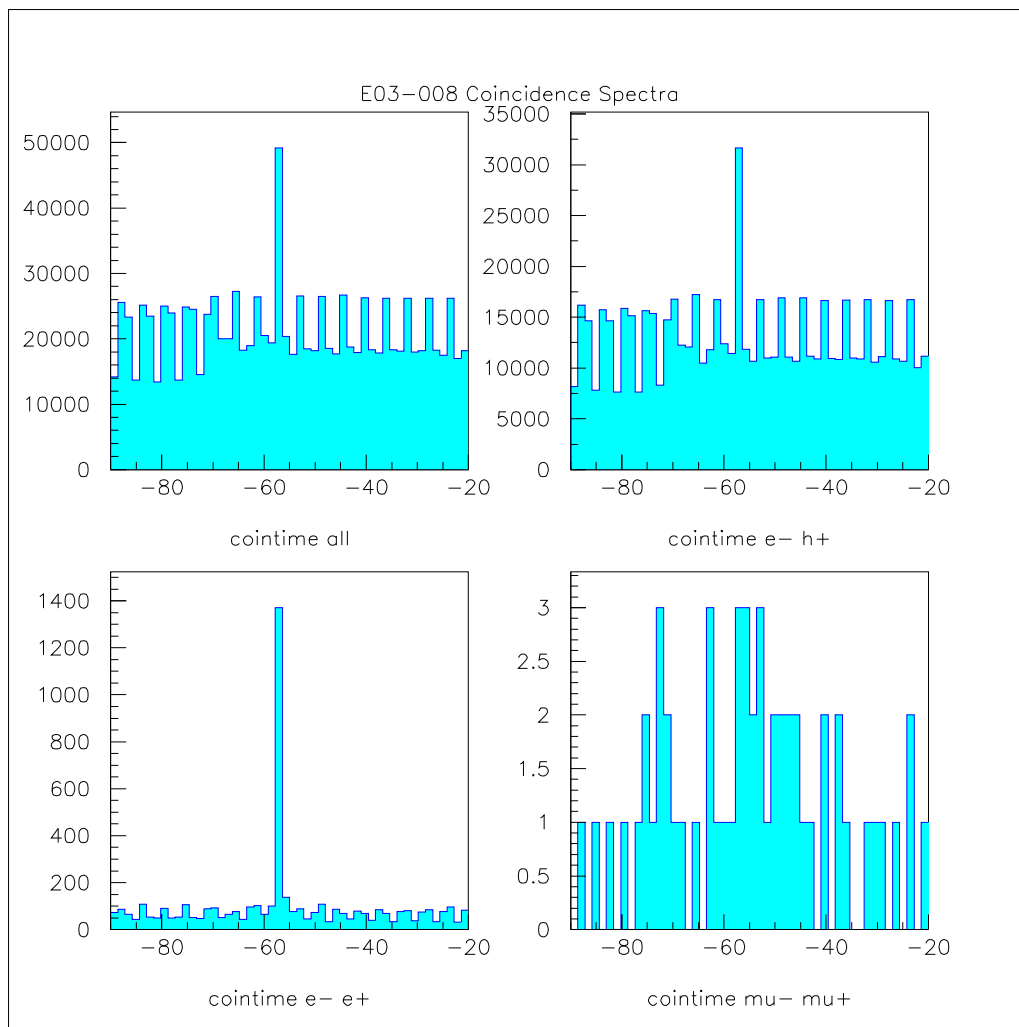


Figure 3.2

Coincidence timings for ω meson

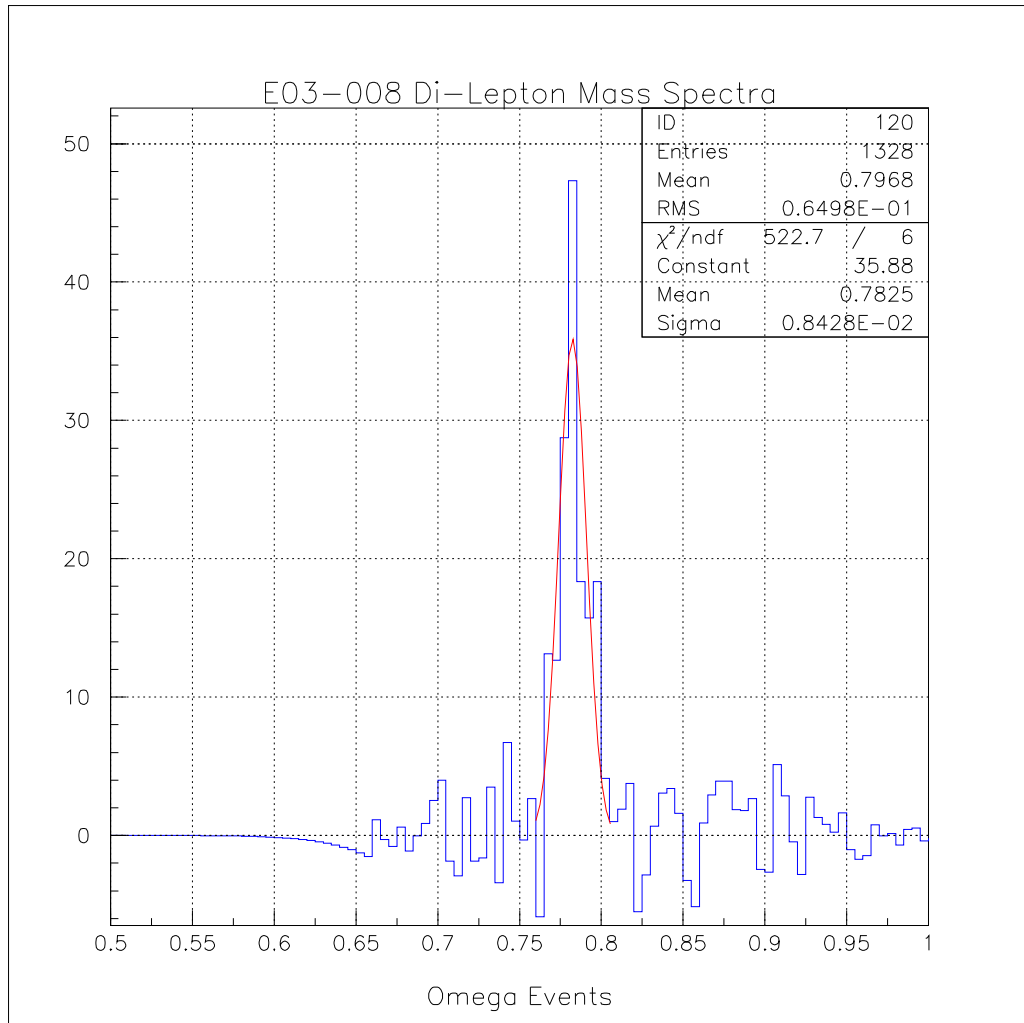


Figure 3.3

Background subtracted events for ω

3.3 Monte-carlo Simulation

The Monte-carlo simulation attempts to reproduce the physical situation for photoproduction and gives satisfactory results(as we will see in the next chapter) and hence is reliable.

The code is designed to simulate only real photons and with appropriate model can simulate any vector meson including, ρ , ω , ϕ and J/ψ . This section will describe the structure of simulation and its features.

3.3.1 Main Event Loop

The main event loop simulates the interaction $\gamma p \rightarrow Vp$, where V is the particular vector meson, by generating the photon and nucleon events with appropriate models as described below. The code then accepts only those events whose center of momentum energy is greater than the photoproduction threshold of that particular vector meson. These events are then weighted by appropriate parameters as described in further sections and finally recorded so as to be analysed by the PAW software. This section now describes the detail structure of simulation and all the tasks in the same order as the code proceeds.

- *Initialisation*

The simulation requires certain initial parameters to start with which are described below,

- *Maximum Photon Energy* This refers to the maximum energy of bremsstrahlung photons and is usually same as the beam energy in the experiment.
- *Number of Events* These are the desired number of events we wish to be recorded in the spectrometer. The code makes more attempts to match this as it is weighted by several other parameters.
- *Particle ID* This refers to the desired vector meson for which the code needs to be simulated. Actually, we specify the mass and width of the particular vector meson.

- *Spectrometer Cuts* This refers to turning on the spectrometer which also simulate the presence of spectrometers. This increases the number of attempts as not all the events generated are recorded by the spectrometer.
 - *t-models* t is the 4-momentum transfer to the target. This parameter provides an option to be run with different t-models. This will be described in detail in the later section.
 - *Cross-section weighting* This parameter provides an option for weighting the number vector meson events by the photoproduction cross-section of that particular vector meson.
- *Bremsstrahlung photon flux*

The high energy electron beam collides with the stationary target and produces high energy photons. The no of photons produced with a beam energy E is given by [13],

$$dk(1/k)\left[\frac{4}{3}(1 - k/E) + (k/E)^2\right] \quad (3.2)$$

where $k = E_\gamma$ is photon energy.

In the simulation, after initialisation, the code generates photon events based on above distribution. This is done by weighting a very accurate uniform random number generator from CERNLIB by the above ditribution.

- *Nucleon model for bound proton* The high energy photons collide with the bound proton to photoproduce a vector meson. In case of J/ψ , the proton must be off-shell for sub-threshold photoproduction. A model is therefore used to take into account the nucleon-nucleon correlations for momentum distribution.
- *Event Selection*

The event selection is done by calculating the center-of-mass energy squared and comparing with threshold energy in center-of-mass. The center-of-mass energy squared is calculated for the interaction $\gamma p \rightarrow Vp$, with p as the bound proton (with nucleon momentum P_p) and incident photon.

$$s = (E_p^2 - P_p^2) + 2E_\gamma E_p - 2E_\gamma P_p \cos\theta \quad (3.3)$$

where θ is angle between the incident photon vector and the nucleon momentum vector. This angle θ is also calculated flat in $\cos\theta$ with uniform random generator.

The threshold energy in a center-of mass is simply given by,

$$s_{th} = (M_V + M_p)^2 \quad (3.4)$$

where M_V is the mass of the particular vector meson and M_p is mass of proton. A vector meson event can be considered to be generated when $s > s_{th}$.

- *Vector meson kinematics*

The generation of vector meson event tells us nothing about kinematical quantities such as the energies, momenta, decay distribution etc. The energy of recoiling proton in the center-of-mass frame is given by,

$$E_{pcm} = \frac{s + M_p^2 - M_j^2}{2\sqrt{s}} \quad (3.5)$$

The center-of-mass energy of the vector meson is simply,

$$E_V = \sqrt{s} - E_{pcm} \quad (3.6)$$

A lorentz boost to above quantities tranform them to lab. These kinematical quantities are set in the code to be recorded as event properties and can be analysed using PAW. The results of these will be demonstrated in next chapter. At this stage, appropriate t -models are introduced to weight the differential cross-section with respect to t as shown in Figure 1.1 and Figure 1.2. These will be discussed in later section.

- *Detection and Recording*

In the experiment, the spectrometers are set in a particular geometry to detect the leptonic decays of the vector meson. The tasks of the code now are to generate the decay events and detect them.

The characteristics of the decay products are, they fly 180° apart in the rest frame of the vector meson. The angular distribution of these leptons can be set in the simulation as flat(isotropic) or weighted by $(1 + \cos^2\theta)$. The kinematical properties of these decays are recorded after a lorentz boost to the lab.

The geometry of spectrometer is simulated by an option in the initialisation called 'spectrometer cuts'. The spectrometer cuts in the code are set by introducing the solid angle of the spectrometer openings to the target. Hence, the events generated over 4π steradians are now weighted by these cuts. The events generated with spectrometer cuts are also used later for acceptance corrections.

Finally, the recording of the events is done by filling histograms of respective quantities. The code then checks over for set quantities such as number of events and loops over until it reaches those events.

3.3.2 Models for t -dependence

The vector mesons show a cross-section dependence in t as can be clearly seen in Figure 1.1 and Figure 1.2 This factor is incorporated in the simulation, while calculating the

vector meson kinematics as was discussed earlier. In this section, these models are presented and the model for ω is presented in detail as it is to be compared with data.

3.3.2.1 *Diffractional t distribution*

Diffractional distribution is modeled in simulation with an exponential cross-section dependence given as $d\sigma/dt = Ne^{bt}$ where, N is normalised events and b is the slope of the exponential distribution. The total number of events to be recorded in the spectrometer are now weighted over this distribution. This model is more realistic and can simulate, for example, the photoproduction of ρ meson as it exhibits diffractional distribution in Figure 1.1.

The diffractional events are generated by calculating,

$$t_{min} = M_V^2 - 2E_\gamma E_V + 2p_\gamma p_V \quad (3.7)$$

$$t_{max} = M_V^2 - 2E_\gamma E_V - 2p_\gamma p_V \quad (3.8)$$

corresponding to $\theta = 0$ and $\theta = \pi$ respectively. The exponential range of the t_{min} and t_{max} is weighted by a random number generator to give a diffractional distribution. The acceptance results from diffractional cross-section will be presented in next chapter.

3.3.2.2 *Diffractional and OPE Model for ω*

This model is simulated on the basis of the paper by [9]. This paper was written for electroproduction of ω based on the theory for photoproduction. Since this thesis deals with only photoproduction, the simplified calculation for $Q^2 = 0$ i.e. for real photons are

presented. According to this paper, the total differential cross-section dependence is the sum of OPE contribution and Diffractive contribution,

1. *One Pion Exchange contribution* The differential cross-section $d\sigma_T^\pi/dt$ for transverse photons, is given by

$$d\sigma_T^\pi/dt = \frac{1}{(P(0)^2 W^2)} G^2 \frac{\Lambda_{\omega\pi}^2}{16} \frac{-t}{(t - m_\pi^2)^2} \frac{(B + C)^2}{-C} F_N F_\omega \quad (3.9)$$

where G^2 is square of the pion-nucleon coupling = 14.6,

$$\Lambda_{\omega\pi}^2 = 96\pi \left(\frac{m_\omega}{(m_\omega^2 - m_\pi^2)} \right)^3 \Gamma_{\omega\pi\gamma} \quad (3.10)$$

with $\Gamma_{\omega\pi\gamma}=0.9$ MeV; $P(0)^2$ are the photon momenta in the hadron c.m.s for real and virtual photons, respectively; m_π, m_ρ, m_ω are the masses of π, ρ and ω respectively; F_N, F_ω are the form-factors for the π -nucleon and $\gamma\pi\omega$ vertices respectively with:

$$F_N = \frac{(1 + (2.9)^2 Q_{NT}^2)}{(1 + (2.9)^2 Q_{NT}^2)} \quad (3.11)$$

where

$$Q_N^2 = \frac{m_\pi^2(m_\pi^2 - 4m_p^2)}{4m_p^2}, \quad (3.12)$$

$$Q_{NT}^2 = \frac{t(t - 4m_p^2)}{4m_p^2} \quad (3.13)$$

$$F_\omega = \frac{U(2.3QF)}{U(2.3QT)} \left(\frac{QT}{QF} \right)^2 \quad (3.14)$$

where

$$U(x) = \frac{[\frac{2x^2+1}{4x^2} \log(4x^2 + 1) - 1]}{2x^2} \quad (3.15)$$

QT is the momentum of the on-shell pion(or γ) in the ω frame. The quantities B, C, N_3 are defined as follows,

$$B = 0.25(m_p^2 - W^2)(m_p^2 + m_\omega^2 - W^2 - t), \quad (3.16)$$

$$C = -0.25(W - m_p)^2(W + m_p)^2 \quad (3.17)$$

$$N_3 = 0.5[W^2 t u - t m_p^2(m_p^2 - m_\omega^2) - m_p^2 m_\omega^4]^{1/2} \quad (3.18)$$

with

$$W^2 + t + u = 2m_p^2 + m_\omega^2 \quad (3.19)$$

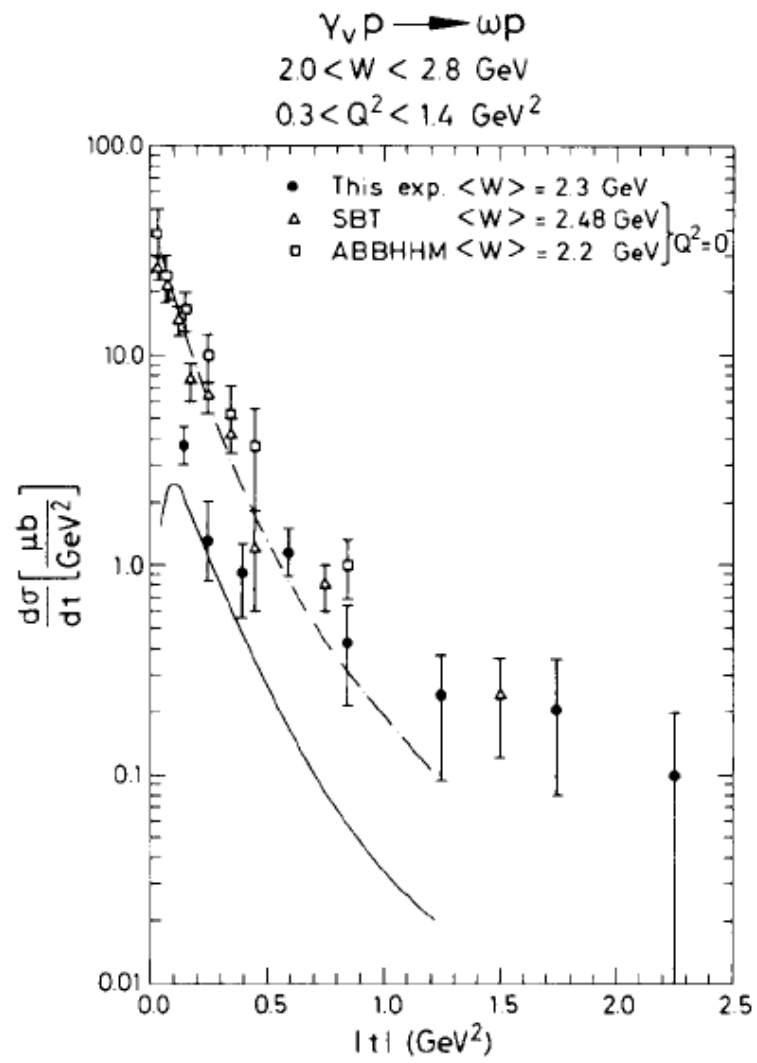


Figure 3.4

t -dependence for OPE and diffraction from [9]

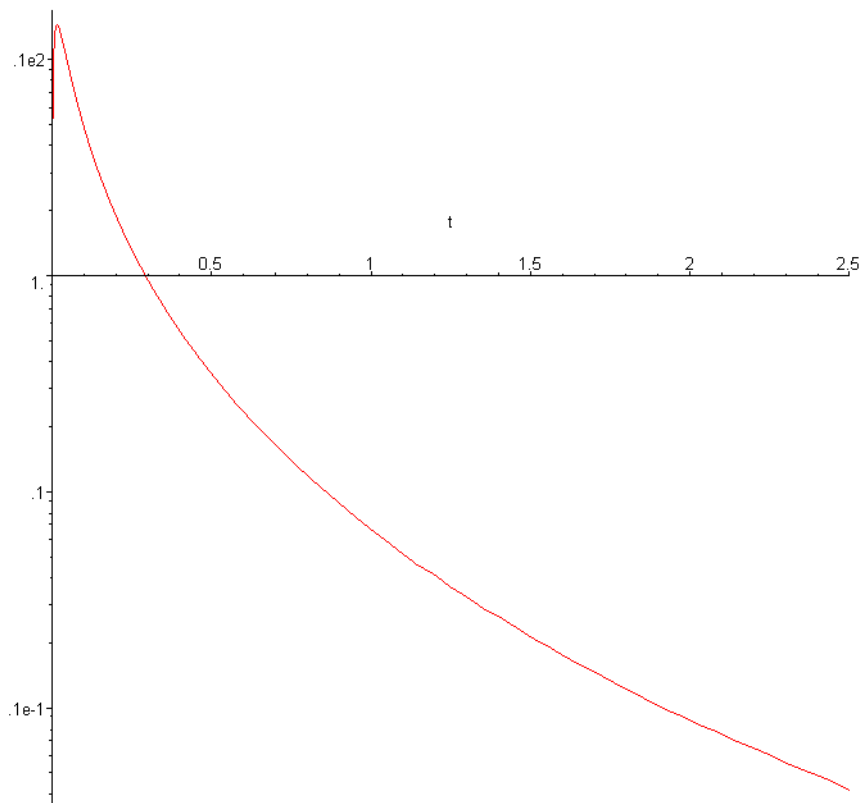


Figure 3.5

Presimulation of OPE and Diffractive model for real photons from [9]

2. *Diffraction Contribution* The diffractive contribution is given by

$$\sigma_D(\mu b) = 9.3 e^{(6.7t)} \left(1 + \frac{1.4}{E_\gamma}\right) \quad (3.20)$$

where

$$E_\gamma = \frac{(W^2 - m_p^2)}{2m_p} \quad (3.21)$$

The results of their models is shown in the Fig 3.4. It must be noted that their model is based for electroproduction and hence $Q^2 \neq 0$.

Now to simulate this model, it is too complicated and inefficient to directly use these relations in the main simulation. Hence, this model was ‘pre-simulated’ in MAPLE to reduce the number of variables to only two. Further, this pre-simulation was based on real photons and it was expected to represent the same fit as used by [9]. The result from MAPLE presimulation is shown in Fig 3.5. The presimulation is able to reproduce the the fit as by [9]. It can also be observed that, over the same range of ‘t’ this curve drops faster than by [9]. This is attributed by the fact this curve is for real photons i.e. $Q^2 = 0$.

3.4 Cross-section for ω Photoproduction

In the simulation, a vector meson event is generated by when $s > s_{th}$. In reality, the cross-section has a photon energy dependence and this factor needs to be taken into account in the simulation. The energy dependence of the cross-section is presented in a paper by [2] and is shown is Fig 3.6.

To incorporate this model, the cross-section dependence was curve fitted in MAPLE by the points given in this paper. Further, the photon energy range for the above fit is

from 2.5 GeV to 3.5 GeV. The significance of this range is only photons produced in this range actually contribute to omega events in the spectrometer. (This is shown in the results section. The appropriate curve fit was found to be Thiele Interpolation and the result is in fig 3.7. This cross-section fit was normalised to unity and normalisation cross-section is given by,

$$\sigma_{normalised} = 6.277 \mu b \quad (3.22)$$

Now, in the simulation, when a vector meson event is generated, the code weights a uniform random number generator to match the above which is normalised. Hence, now we have events which are weighted over Ballam data.

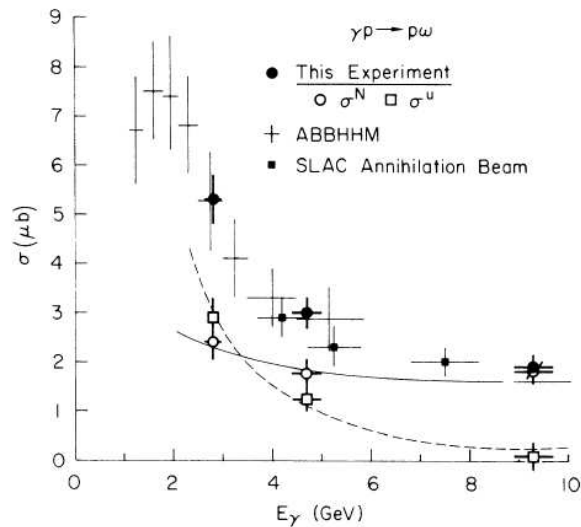


Figure 3.6

Cross-section dependence on Photon Energy [2]

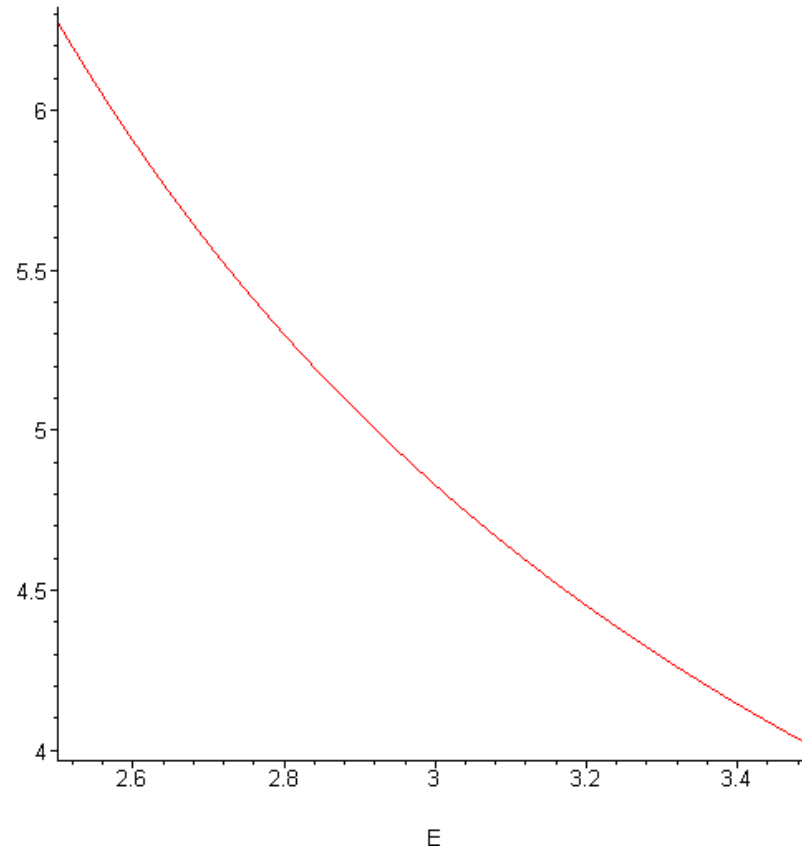


Figure 3.7

Curve fitted Ballam data

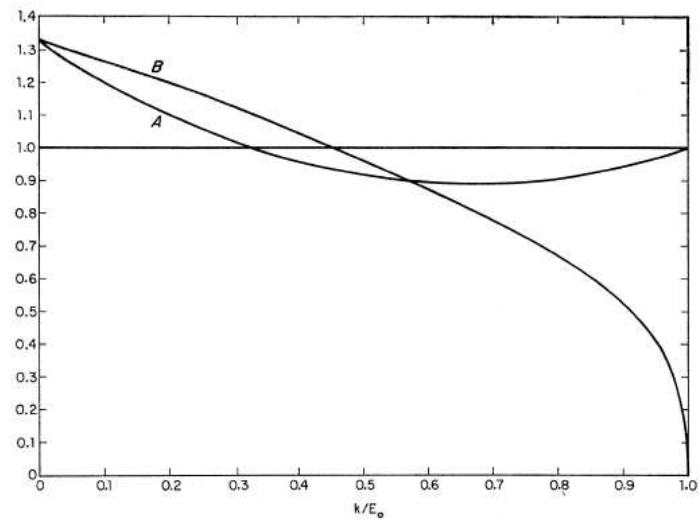


Figure 3.8

Bremsstrahlung Spectrum [13]

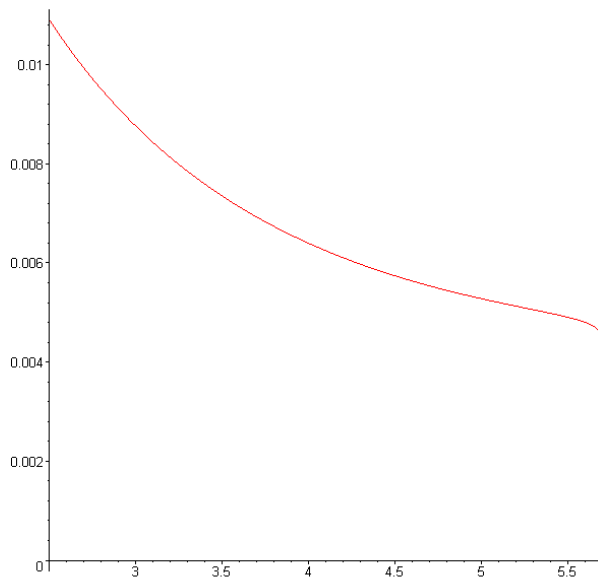


Figure 3.9

Bremsstrahlung spectrum from MAPLE simulation

3.5 Bremsstrahlung Photons Calculation

The passage of high energy electrons through a stationary target produces a radiation shower called bremsstrahlung radiation which produces high energy photons in the target. The bremsstrahlung spectrum of these photons is considered in a classic paper by [13] and the photon flux is given by,

$$I_{\gamma} = e^{-(7/9)t} \int_0^t \frac{e^{(7/9)t'}}{\Gamma(1 + \frac{4}{3}t')} \left(\ln \frac{1}{u}\right)^{\left(\frac{4}{3}t'\right)} \times \left[u + \sum_{n=0}^{\infty} \frac{1}{n!(n + (\frac{4}{3}t' + 1))} \left[\frac{4}{3}(-1)^n - u^2\right] \times \left(\ln \frac{1}{u}\right)^{n+1}\right] dt' \quad (3.23)$$

where $u = k/E_0$ and This refers to equation (24) in [13]. The result of this relation as plotted by Tsai-Whitis is as in fig 3.8.

The calculation is used to find out the photon spectrum and thereof knowing the total number of photons produced. This is required to predict the number of omega events and to compare it with experimental results. The above relations were simulated in MAPLE to find out the probability of finding a photon in a particular photon energy range namely between 2.5 GeV and 3.5 GeV. It is shown later that only omega events corresponding to these energies make it into the spectrometer and hence need to be considered. The results from the MAPLE simulation is shown in fig 3.9.

The horizontal axis is photon energy and vertical axis the photon spectrum. The above plot is integrated over the photon energies from 2.5 GeV to 3.5 GeV, which tells us the probability of finding a photon between 2.5 GeV and 3.5 GeV with electron beam energy of 5.7 GeV.

$$I_{\gamma} = 0.0215 \quad (3.24)$$

We now proceed to calculate the total number of photons produced in the experiment. From experimental data, the total no of electrons with energy 5.7 GeV collided with the target are,

$$N_e = 8.467 \times 10^{17} \quad (3.25)$$

The total no of photons produced are given by,

$$N_\gamma = I_\gamma \times N_e \quad (3.26)$$

This gives $N_\gamma = 9.127 \times 10^{15}$

CHAPTER IV

RESULTS AND DISCUSSION

This chapter will present the results from the simulations and calculations for number of ω events based on the various t -models. Further analysis of cross-section events and photon energy spectrum will demonstrate the reliability of the simulation.

4.1 Acceptance Calculations and t -model Results

Acceptance refers to the acceptance of the spectrometers which is defined here as,

$$\text{Acceptance } (A_{model}) = \frac{\text{Number of events in spectrometers}}{\text{Total Number of vector meson events generated}}$$

In the laboratory, the spectrometers are located at a particular angle from beam line and are able to detect only a fraction of the vector meson events. The code attempts to simulate this and these results will be used later for predicting number of events based on the acceptance given by the code. The code has been run for 100 events in the spectrometer for all cases, hence is numerator in above ratio is always 100.

4.1.1 Diffractive Model

The diffractive model is characterised by an exponential tail as can be seen in the top of Figure 4.1. One might recall Figure 1.1 which also possess similar feature. For this

model and with Ballam cross-section fit, the total number of ω events the code had to generate were 193529 to have 100 events in the spectrometers.. The acceptance is given by,

$$A_{diffraction} = \frac{100}{193529} = 5.167 \times 10^{-4} \quad (4.1)$$

4.1.2 OPE and Diffractive model

This t distribution resulting from OPE and diffractive model is shown in bottom of Figure 4.2. One can immediately observe the forward peak characteristic in OPE which was the characteristic of one particle exchange model as discussed in section 1.3.2. This due to presence of a pole at $t = m_{\pi}^2$ which is in general the particle exchanged in the single particle exchange model. Further the diffractive characteristics as in section 4.1.1 are expected to approximate the OPE effect as OPE is simply sharp peaked. This fact becomes clear on the basis of several factors which we will see as the acceptance, cross-section and photon spectrum of OPE and diffractive models.

The plot obtained below represents the differential cross-section in t as given by [9] which was simplified to two variables using MAPLE and then“fed”to the main simulation. The total number of ω events the code generated for this model were 206931. The acceptance is given by,

$$A_{OPE+diffraction} = \frac{100}{206931} = 4.835 \times 10^{-4} \quad (4.2)$$

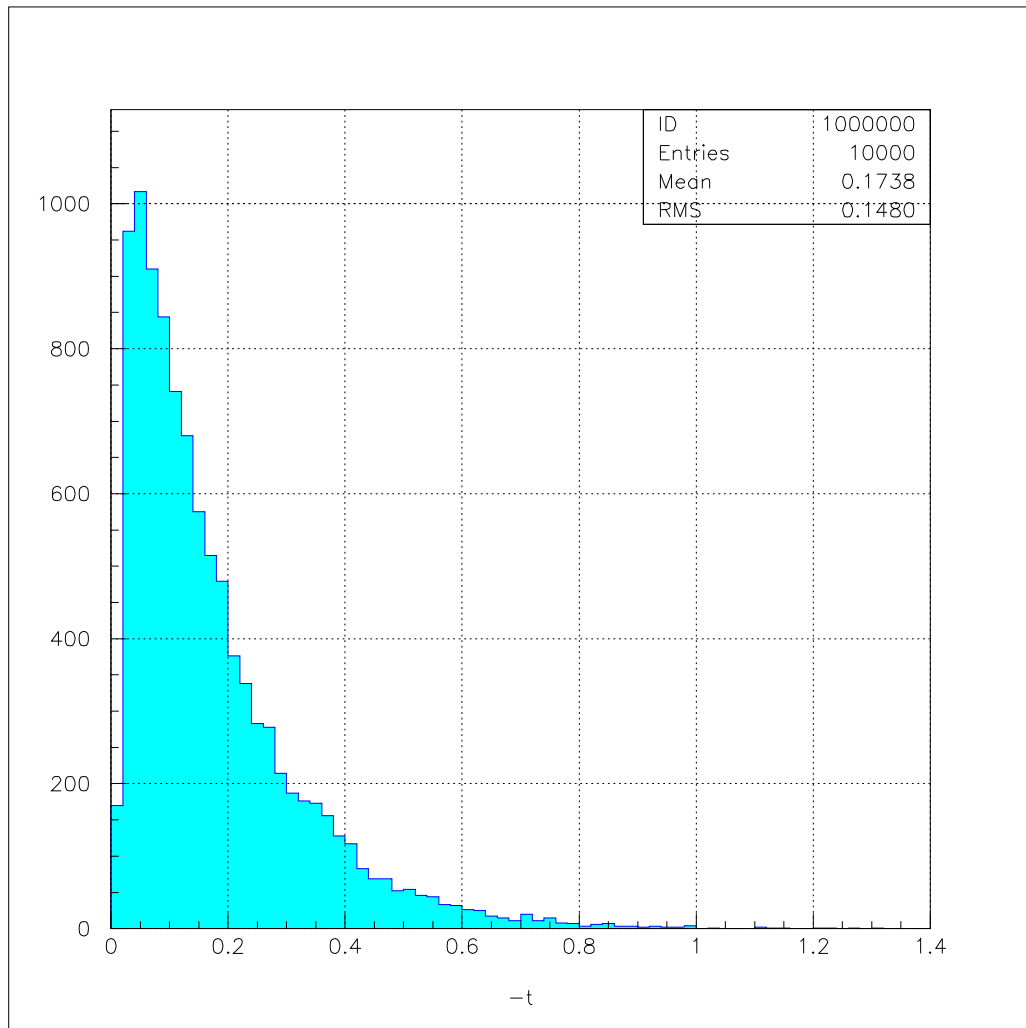


Figure 4.1

Diffractive t distribution

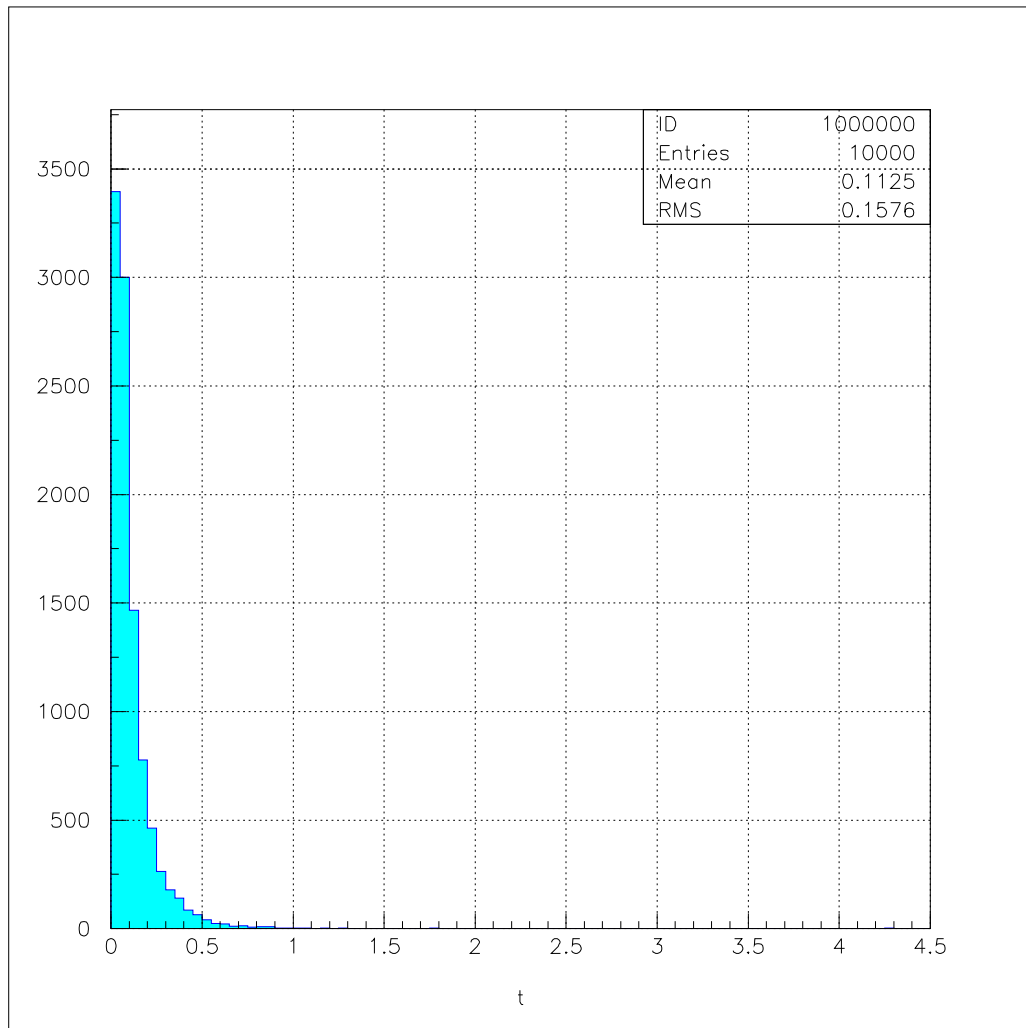


Figure 4.2

OPE+Diffractive t distribution

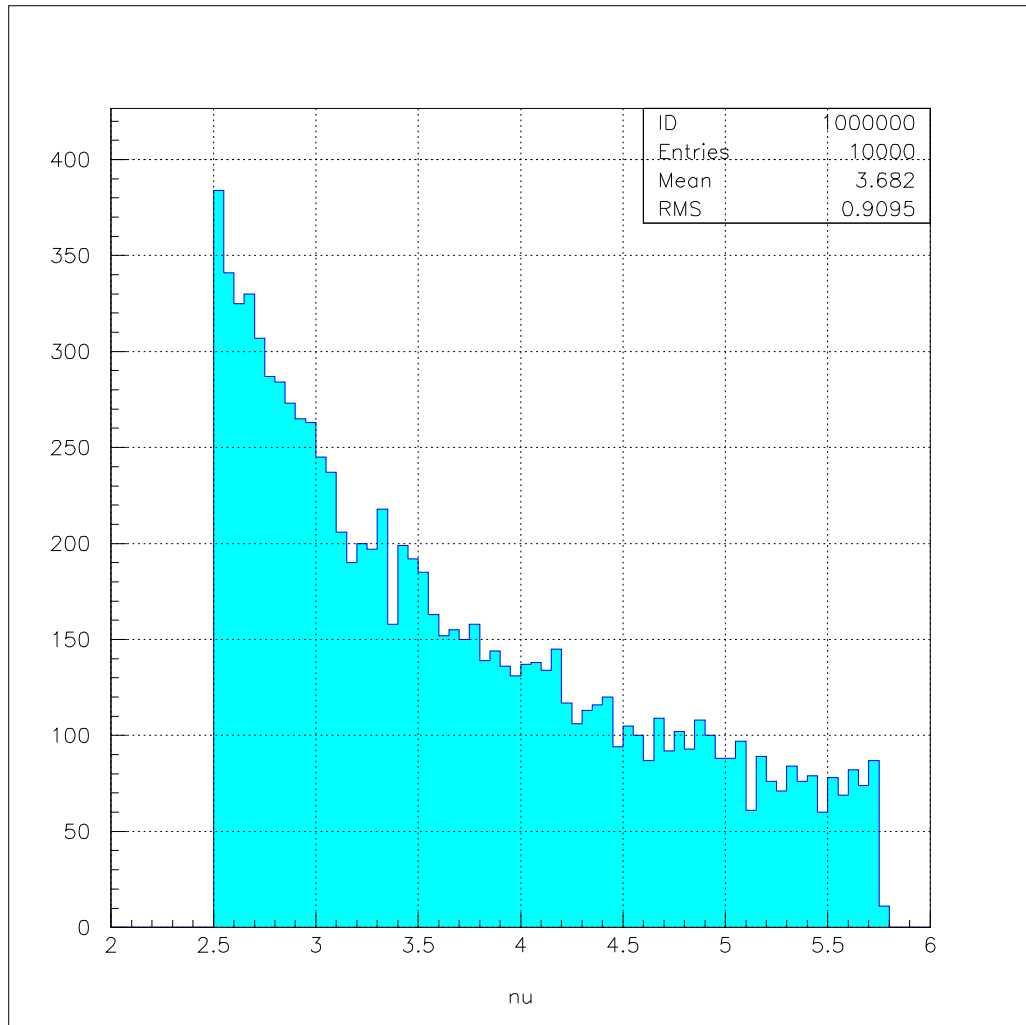


Figure 4.3

Photon Spectrum without Spectrometer cuts for Diffractive model

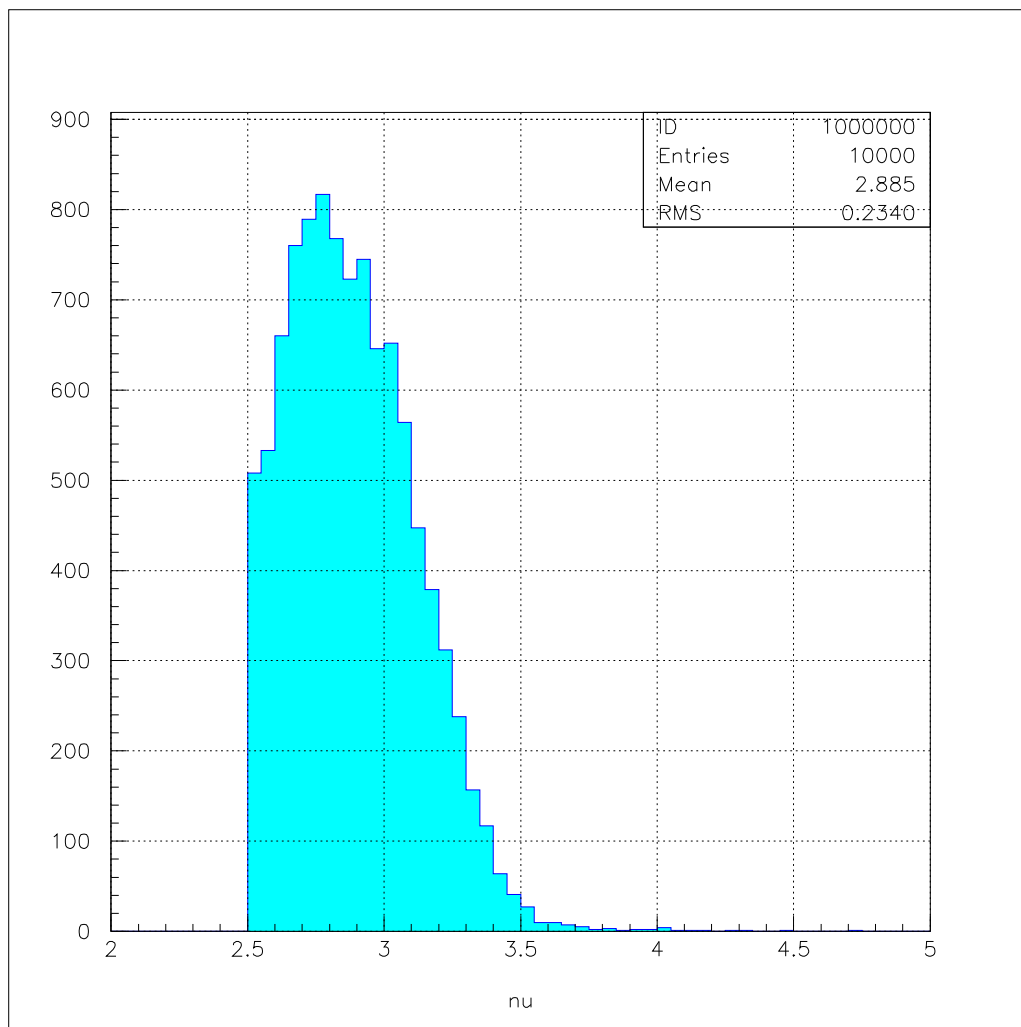


Figure 4.4

Photon Spectrum including Spectrometer cuts for Diffractive model

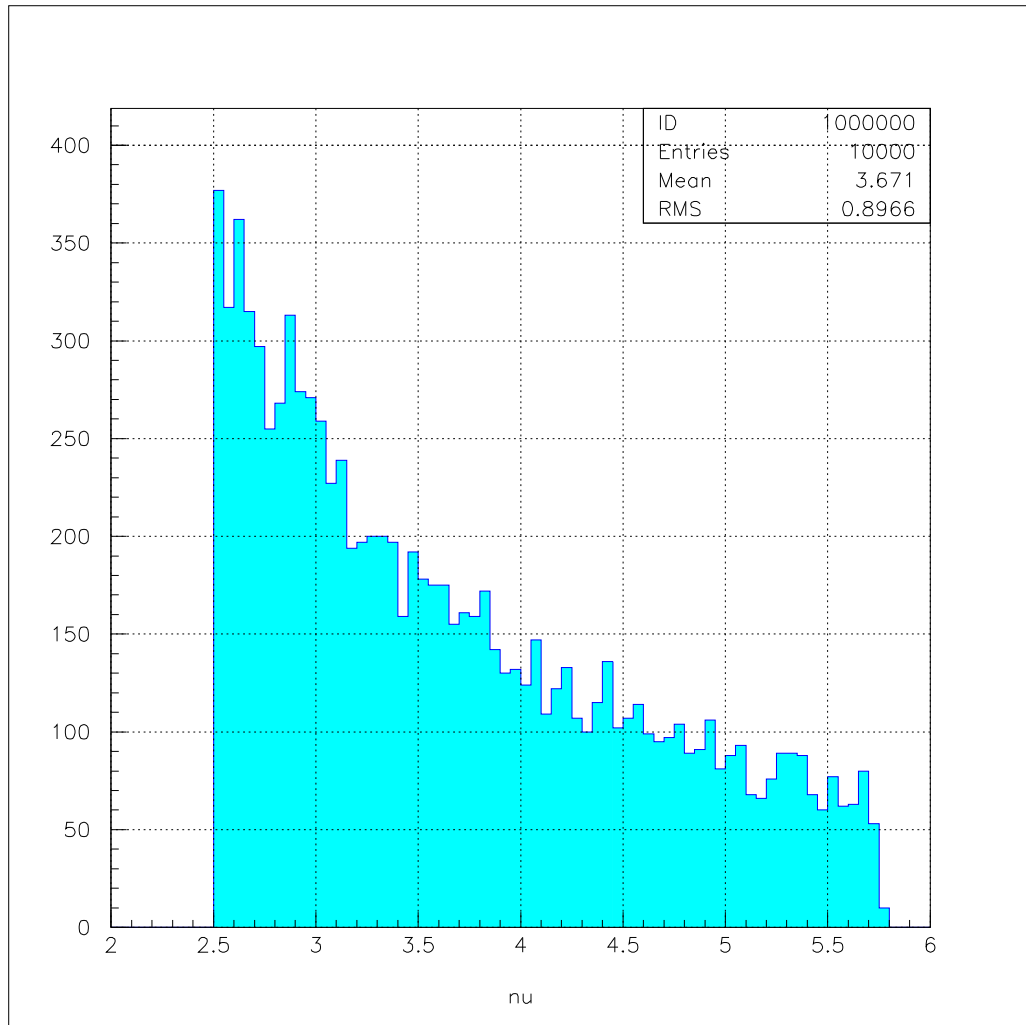


Figure 4.5

Photon Spectrum without Spectrometer cuts for OPE+Diffractive model

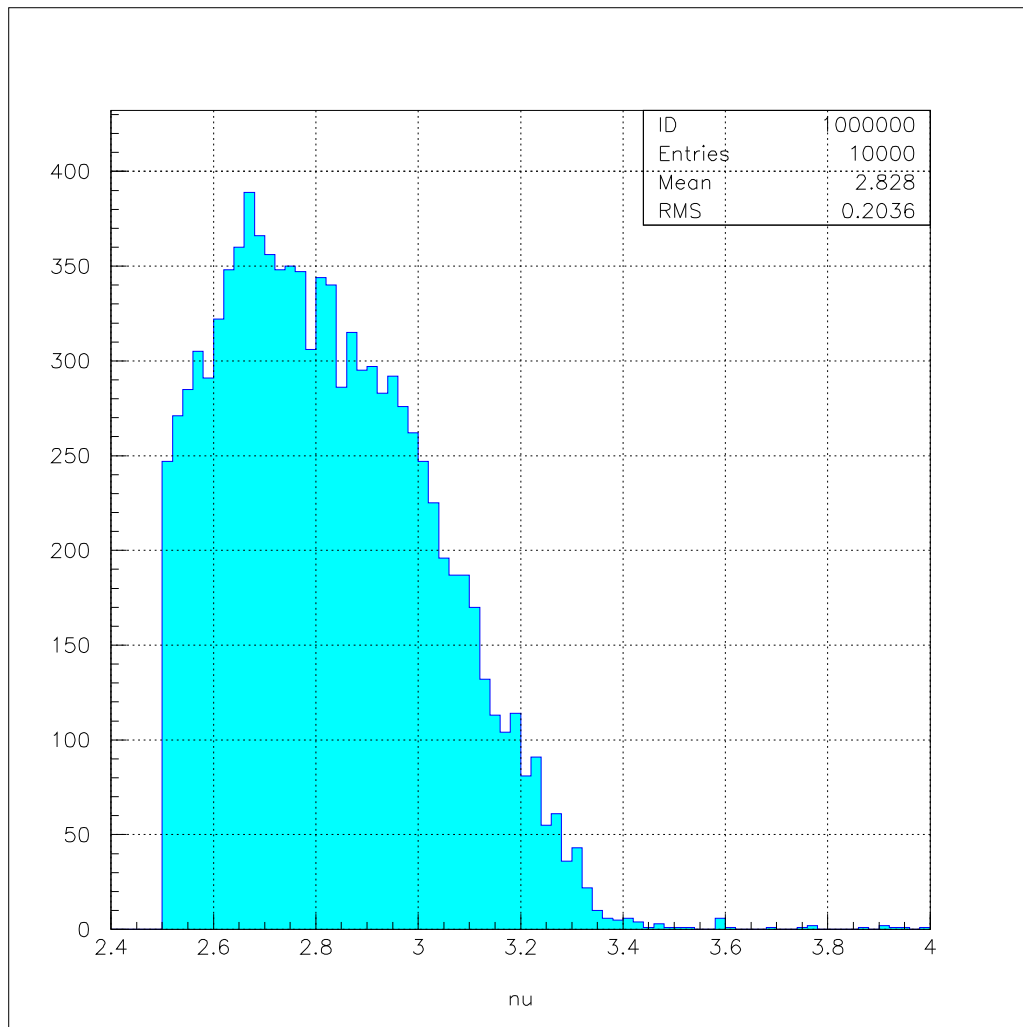


Figure 4.6

Photon Spectrum including Spectrometer cuts for OPE+Diffractive model

4.2 Photon Spectrum

This section shows results of the photon spectrum from the simulation which refers to the bremsstrahlung photon spectrum in the laboratory. The plots in Figure 4.2 show the effect of the spectrometer cuts on the spectrum. The photon spectrum after applying the spectrometer cuts tells us about the energy range of photons that make it into spectrometer. This range can be clearly seen to be from 2.5 GeV to 3.5 GeV. This serves an important simplification in such a way that, since we now know that only photons from 2.5 GeV to 3.5 GeV make it into the spectrometer, the photon spectrum in Tsai and Whitis needs to be integrated only for this range. For the same reason, the Ballam cross-section is considered only from 2.5 GeV and 3.5 GeV, as considering the entire spectrum will result in inefficiency and inaccuracy.

The effect of diffractive and OPE+diffractive model seem not to affect the photon spectrum, since the 'peaked characteristics' of these models is expected to have similar behaviour qualitatively.

As a check, one can also observe the effect of Ballam cross-section on the photon spectrum, the number of photon events tend to decrease with the photon energy meaning there are lesser omega events with higher photon energy.

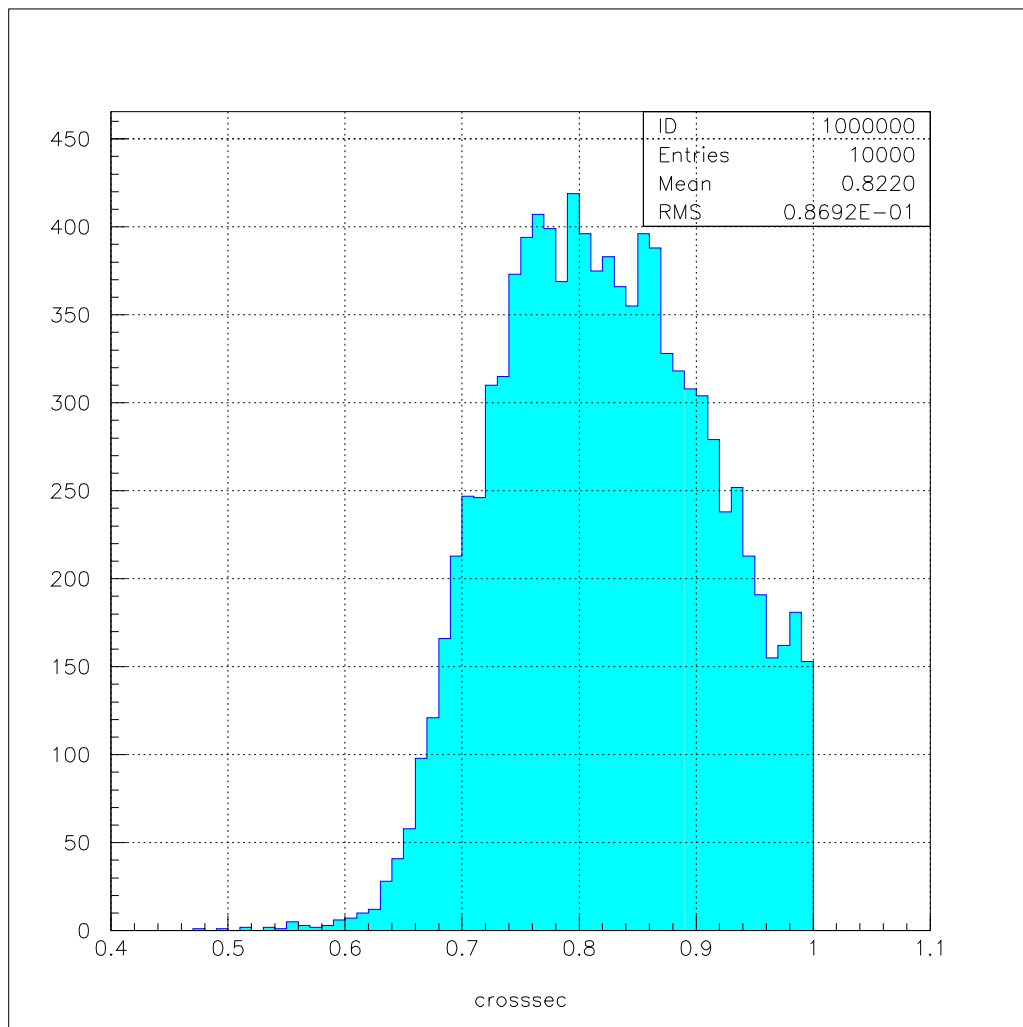


Figure 4.7

Cross-section results for Diffractive model

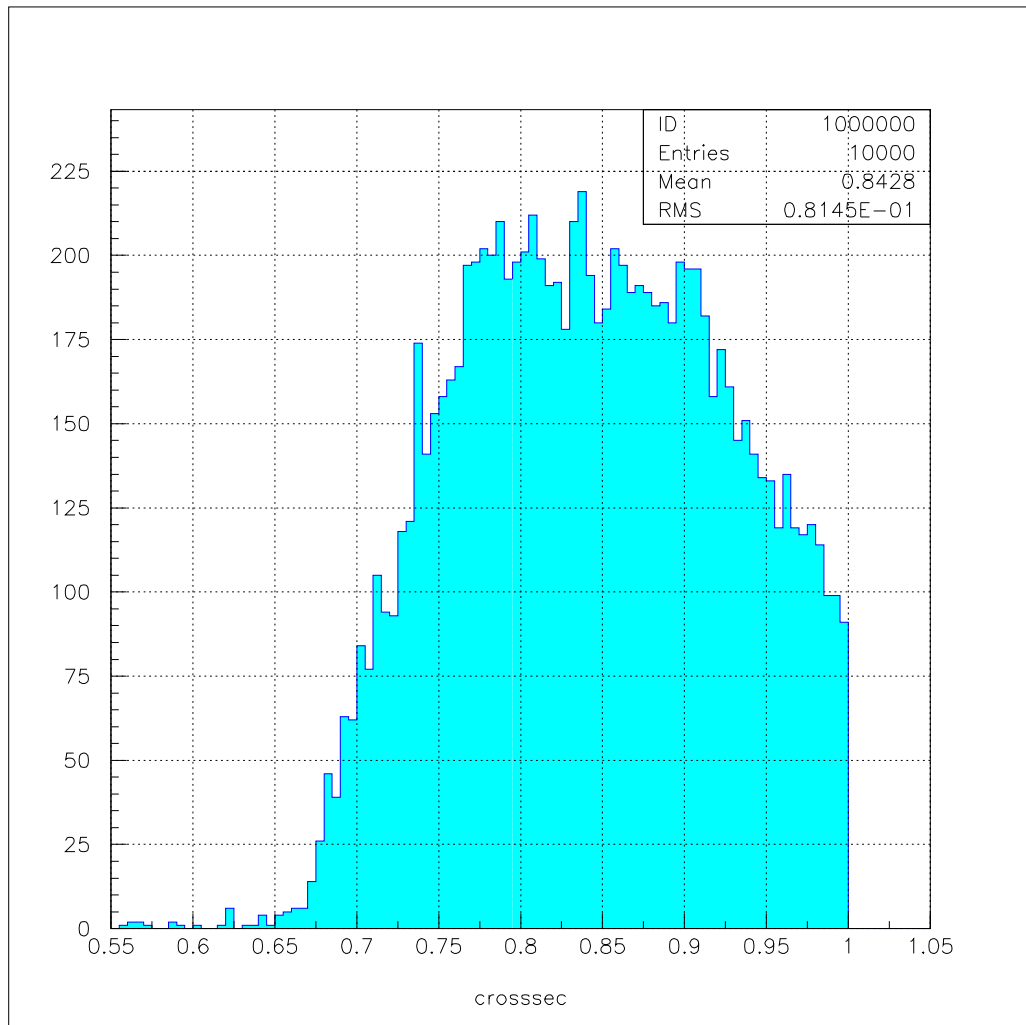


Figure 4.8

Cross-section results for OPE+Diffractive model

4.3 Cross-section Calculations

The simulation results for Ballam cross-section are presented here and further this is used to obtain the mean value of cross-section which will be later used to calculate the number of omega events.

Figure 4.4 shows cross-section events for Diffractive and OPE+diffractive models. One might expect larger number of events for higher cross-section which is contrary to the plots. The drop in the cross-section is due to the spectrometer cuts which is seen from the plots without spectrometer cuts.

The cross-section in the simulation is normalised to unity, where the normalisation factor was calculated in section 3.4. The cross-section calculations for the two models is as below,

1. *Cross-section for Diffractive model* The mean value of the cross-section is obtained from the top plot of Figure 4.4.

$$\sigma_{diff} = 0.822 \mu b \quad (4.3)$$

The normalised cross-section from section 3.4 is $\sigma_{norm} = 6.277 \mu b$. Hence, the total cross-section is given by,

$$\sigma_{tot} = \sigma_{diff} \sigma_{norm} = 5.15 \mu b \quad (4.4)$$

2. *Cross-section for OPE+Diffractive model* The mean value of the cross-section is obtained from the bottom plot of Figure 4.4.

$$\sigma_{diff} = 0.8428 \mu b \quad (4.5)$$

The total cross-section is given by,

$$\sigma_{tot} = \sigma_{diff} \sigma_{norm} = 5.29 \mu b \quad (4.6)$$

4.4 Number of ω Events

In the laboratory, the experiment was conducted for five runs with known parameters such as the beam current, total beam charge, target configuration. The number of ω events are calculated from a simple relation from first principles in scattering as,

$$N_{\omega} = \frac{\sigma_{\omega} N_0 \rho t N_{\gamma}}{A} \quad (4.7)$$

where,(The target in this experiment was 3% Be₉)

- σ_{ω} is the photoproduction crosssection for ω from previous section,
- N_0 is Avogadro's number,
- ρ is density of target = 1.848 gm/cm³,
- t is thickness in radiation length = 1.06 cm for 3% r.l.
- N_{γ} Number of incident photons as calculated in section 3.5
- A is number of nucleons = 9 for Be

Now for Diffractive model the number of events are given by

$$N_{\omega} = 5.532 \times 10^{10} \quad (4.8)$$

These are now corrected for the acceptance of the spectrometer A_{diff} and the branching ratio of omega which is = 7.5×10^5

Hence the total Number of ω events predicted by from the simulation are,

$$N_{\omega diff} = 1863events \quad (4.9)$$

The number of events for OPE and Diffractive are given by,

$$N_{\omega} = 5.6831 \times 10^{10} \quad (4.10)$$

The total events after acceptance correction and branching ratio is,

$$N_{\omega+OPE} = 1923 \text{events} \quad (4.11)$$

4.5 Conclusions and Future Work

Based on the reasonable agreement between the monte-carlo prediction of the number of omega events with actual data, the monte-carlo is verified. In future, it will be used to determine the upper limit to the J/ψ photoproduction cross-section from the null result of sub-threshold experiment. In addition, it will be used in the planning of future studies for the Jefferson lab high energy upgrade.

REFERENCES

- [1] J. R. Arrington, *Inclusive electron scattering from nuclei at $x > 1$ and high Q^2* , doctoral dissertation, CALTECH, 1998.
- [2] J. Ballam et al., “Vector-Meson Production by Polarized Photons at 2.8, 4.7, 9.3 GeV,” *Physical Review D*, vol. 7, no. 11, June 1973.
- [3] T. H. Bauer, R. D. Spital, D. R. Yennie, and F. M. Pipkin, “The hadronic properties of the photon in high-energy interactions,” *Review of Modern Physics*, vol. 50, no. 2, April 1978.
- [4] S. J. Brodsky, E. Chudakov, P. Hoyer, and J. M. Laget, “Photoproduction of charm near threshold,” *Phys. Lett. B498*, Nov 2000.
- [5] C. Caso, “Particle Data Group,” .
- [6] J. Dunne, “Hadron-05,” *Hadron-05*, 2005.
- [7] D. Dutta, *The (e, e', p) Reaction Mechanism in the Quasi-Elastic Region*, doctoral dissertation, Northwestern University, Evanston, Illinois, June 1999.
- [8] H. Frauenfelder and E. M. Henley, *Subatomic Physics*, 2 edition, Prentice Hall, New Jersey, 1991.
- [9] P. Joos et al., “ ω meson production by virtual photons,” *Nuclear Physics B122*, , no. 365-382, 1977.
- [10] D. Meekins, *Coherent π^0 photoproduction on the deuteron*, doctoral dissertation, College of William and Mary, Williamsburg, VA, 1996.
- [11] M. I. Niculescu, *Inclusive Resonance Electroproduction data from hydrogen and deuterium and studies of quark-hadron duality*, doctoral dissertation, Hampton University, Hampton, VA, May 1999.
- [12] M. L. Perl, “High Energy Hadron Physics,” 1974.
- [13] Y. S. Tsai and V. Whitis, “Thick-Target Bremsstrahlung and Target Considerations for Secondary-Particle Production by Electrons,” *Physical Review*, vol. 149, no. 4, September 1966.

APPENDIX
THE MONTE-CARLO CODE

```

      Program photon
C
      implicit none
C
      integer nwpawc,i,ink,lim,j,icycle,istat,count,irlu
      integer N      ! step size for event # print statement
      parameter (nwpawc=200000)
      real*4 h(nwpawc)
      common/pawc/h
      integer*4 nb_events,iocode,decay_ang_dep,nb_attempts,t_dep
      logical mono_E,finished
      character*4 extension
      character*22 filename
      character*4 targ
      real*4 Nk_dev_range,Nk_dev,Nk_min,Nk_max,Nk
      real*4 brem_dev_range,brem_dev,brem_min,brem_max,nu
      real*4 Pp(4),Ppcm(4),Pg(4),Pgcm(4),beta(4),betasq,dir(3)
      real*4 Pprf(3),Pgrf(4)
      real*4 Ep,Eppcm,Ejcm,s,sth,theta,phi
      real*4 pcm(4,2),pmul,thmul,phmul,pmu2,thmu2,phmu2
      real*4 thmul_s,thmu2_s,phmul_s,phmu2_s
      real*4 Mp,Mj,pi,mj_width,mj0
      real*4 b,z,p,m,q
      real*4 alpha,random,ran_k,t_min,t_max,t_dev_range,t_dev,t,t_new
      real*4 pppcm,pjcm,pjcm_v(4),pgcm_mag
      real*4 thjcm,phjcm
      real*4 Ejlab,Pjlab,Pjlab_v(4),thjlab,phjlab
      real*4 k_cutoff      ! splits the nk dist of nuclear matter into 2 regions
      real*4 x_cutoff      ! prob. of k being in region 1 (depends on max Egamma)
      real*4 flat_int
      real*4 exp_int
      real*4 norm_flat
      real*4 norm_exp
      real*4 mjlow, mjhi
      real*4 x(1001),y(1001),slope
      real*4 raddeg/57.29578/
      real*4 r,XX(200),XRAN
      real*4 YY(200),YRAN
      real*4 ZZ(200),ZRAN,crosssection,rand
      real*4 sig,sig_min,sig_max,sig_dev
      external breit_wigner
      real*4 breit_wigner
      external diff
      real*4 diff
      external ballamfit
      real*4 ballamfit
      COMMON s
      real*4 tftot, rsteps, x2low, x2high, xlow, xhigh
      integer*4 ifunc,ierr
      real*4 uncert, x2, x3, tftot1, tftot2, xrange
      parameter (rsteps = 0.0002)
C
      COMMON/FUNINT/TFTOT

      logical spect_cuts,record_ntuple,weight,keep
      real*4 sos_p0,sos_p_range,sos_th0,sos_th_range,sos_ph0,
>      sos_ph_range, hms_p0,hms_p_range,hms_th0,hms_th_range,
>      hms_ph0,hms_ph_range
      common/spect_cuts/sos_p0,sos_p_range,sos_th0,sos_th_range,
>      sos_ph0,sos_ph_range,hms_p0,hms_p_range,

```



```

>          hms_th0,hms_th_range,hms_ph0,hms_ph_range
C
integer nb_var
parameter (nb_var=32)
real*4 angs(nb_var)
common/ntup/angs

character*8 tags(nb_var)
data angs/nb_var*0.0/

data tags/'Nu','Nk','Thp','Php','s','Pjcm','Ejcm','THjcm','PHjcm',
>         'PjLab','EjLab','ThjLab','PhjLab','z','t','tprime',
>         'Pmu_cm','Thmu_cm','Phmu_cm','Pmu1_l','Thmu1_l',
>         'Phmu1_l','Pmu2_l','Thmu2_l','Phmu2_l','Egam_rf','Mj',
>         'Phsmul','Thsmul','Phsmu2','Thsmu2','crosssection'/
C

common/const/pi,raddeg,mj,mj0,mj_width

data pi/3.1415927/
data Mp/0.93827/
data Nk_min/0.0/
data Nk_max/1.0/
data brem_min/4.0/
data brem_max/8.0/
data k_cutoff/0.295/
data alpha/7.6753/
data norm_exp/47.3631/
data norm_flat/117.0/

external rndm
real*4  rndm
real    rlu
C          Read input parameters

open(20,file='input.dat',iostat=iocode,status='old')
read(20,*) brem_max
read(20,*) nb_events
read(20,*) mono_E
read(20,*) extension
read(20,*) targ
read(20,*) b
read(20,*) mj
read(20,*) mj_width
read(20,*) N
read(20,*) decay_ang_dep
read(20,*) t_dep
read(20,*) spect_cuts
read(20,*) weight
close(20)
if(spect_cuts) then
  if(mj.eq.3.098) then
    open(20,file='spect_cuts_jpsi.dat',
>         iostat=iocode,status='old')
  elseif(mj.eq.1.02) then
    open(20,file='spect_cuts_phi.dat',
>         iostat=iocode,status='old')
  elseif(mj.eq.0.782) then
    open(20,file='spect_cuts_omega.dat',
>         iostat=iocode,status='old')
  endif
read(20,*) sos_p0
read(20,*) sos_p_range

```

```

        read(20,*) sos_th0
        read(20,*) sos_th_range
        read(20,*) sos_ph0
        read(20,*) sos_ph_range
        read(20,*) hms_p0
        read(20,*) hms_p_range
        read(20,*) hms_th0
        read(20,*) hms_th_range
        read(20,*) hms_ph0
        read(20,*) hms_ph_range
        close(20)
        sos_th0 = sos_th0/raddeg
        sos_th_range = sos_th_range/raddeg
        sos_ph0 = sos_ph0/raddeg
        sos_ph_range = sos_ph_range/raddeg
        hms_th0 = hms_th0/raddeg
        hms_th_range = hms_th_range/raddeg
        hms_ph0 = hms_ph0/raddeg
        hms_ph_range = hms_ph_range/raddeg
        record_ntuple=.false.

    else
        record_ntuple=.true.
    endif

    open(20,file='int_'//targ//'_500.dat',iostat=iocode,status='old')
    do i=1,501
        read(20,*)y(i),x(i)
CX write(6,*)x(i),y(i)
    enddo
    close(20)
CX filename = 'photon_'//targ//'_//extension//'.hbook'

    if(mj.eq.3.098) then
        brem_min = brem_max-0.3 ! I'm using a small E bin to compare w/ est.
    elseif(mj.eq.1.02) then
        brem_min = brem_max-0.1
    elseif(mj.eq.0.782) then
        brem_min = 2.5
    endif

CX
C          Book histograms

    call hlimit(nwpawc)
    if(mj.eq.3.098) then
        call hropen(2,'jpsi','jpsi_'//targ//'_//extension//'.rz',
>         'N',1024,istat)
    elseif(mj.eq.1.02) then
        call hropen(2,'jpsi','phi_'//targ//'_//extension//'.rz',
>         'N',1024,istat)
    elseif(mj.eq.0.782) then
        if(t_dep.eq.0)then
            call hropen(2,'jpsi','omeg0_'//targ//'_//extension//'.rz',
>             'N',1024,istat)
        elseif(t_dep.eq.1)then
            call hropen(2,'jpsi','omeg1_'//targ//'_//extension//'.rz',
>             'N',1024,istat)
        elseif(t_dep.eq.2)then
            call hropen(2,'jpsi','omeg2_'//targ//'_//extension//'.rz',
>             'N',1024,istat)
        endif
    else
        call hropen(2,'jpsi','unkn_'//targ//'_//extension//'.rz',

```

```

>          'N',1024,istat)
endif
C    call hropen(3,'hbook',filename,'N',1024,istat)
    call hbookn(9,'jpsi',nb_var,'jpsi',2000,tags)

    call hbook1(100,'Photon spectrum',100,brem_min,brem_max,0.)
    call hbook1(101,'Nk spectrum',100,nk_min,nk_max,0.)
    if(brem_max.gt.8.5) then
        call hbook1(102,'theta',200,0.0,180.,0.)
        call hbook1(108,'theta thres',200,0.0,180.0,0.)
    else
        call hbook1(102,'theta',100,90.0,180.,0.)
        call hbook1(108,'theta thres',100,90.0,180.0,0.)
    endif
    call hbook1(103,'phi',100,-180.,180.,0.)
    if(mj.eq.3.098) then
        call hbook1(104,'s',100,10.,20.,0.)
        call hbook1(105,'s thres',100,10.,20.,0.)
        call hbook1(110,'Eff. Photon E ',100,8.0,24.0,0.)
        call hbook1(111,'Jpsi CM Energy ',100,3.0,4.0,0.)
        call hbook1(112,'Jpsi CM momentum ',100,0.,2.0,0.)
        call hbook1(115,'Jpsi Lab Energy ',100,3.0,8.0,0.)
        call hbook1(116,'Jpsi Lab momentum ',100,0.,8.0,0.)
        call hbook1(120,'Muon1 Lab momentum ',100,0.,8.0,0.)
        call hbook1(123,'Muon2 Lab momentum ',100,0.,8.0,0.)
        call hbook2(300,'Lab P vs Lab theta',100,0.,180.,100,0.,9.0,30)
    elseif(mj.eq.1.02) then
        call hbook1(104,'s',100,2.,8.,0.)
        call hbook1(105,'s thres',100,2.,8.,0.)
        call hbook1(110,'Eff. Photon E ',100,1.5,4.0,0.)
        call hbook1(111,'Jpsi CM Energy ',100,1.0,3.0,0.)
        call hbook1(112,'Jpsi CM momentum ',100,0.,0.5,0.)
        call hbook1(115,'Jpsi Lab Energy ',100,1.0,3.0,0.)
        call hbook1(116,'Jpsi Lab momentum ',100,0.,3.0,0.)
        call hbook1(120,'Muon1 Lab momentum ',100,0.,1.6,0.)
        call hbook1(123,'Muon2 Lab momentum ',100,0.,1.6,0.)
        call hbook2(300,'Lab P vs Lab theta',100,0.,180.,100,0.,1.6,30)
    elseif(mj.eq.0.782) then
        call hbook1(104,'s',100,2.,8.,0.)
        call hbook1(105,'s thres',100,2.,8.,0.)
        call hbook1(110,'Eff. Photon E ',100,1.5,4.0,0.)
        call hbook1(111,'Jpsi CM Energy ',100,1.0,3.0,0.)
        call hbook1(112,'Jpsi CM momentum ',100,0.,0.5,0.)
        call hbook1(115,'Jpsi Lab Energy ',100,1.0,3.0,0.)
        call hbook1(116,'Jpsi Lab momentum ',100,0.,3.0,0.)
        call hbook1(120,'Muon1 Lab momentum ',100,0.,1.6,0.)
        call hbook1(123,'Muon2 Lab momentum ',100,0.,1.6,0.)
        call hbook2(300,'Lab P vs Lab theta',100,0.,180.,100,0.,1.6,30)
    endif
    call hbook1(106,'Nk thres',100,nk_min,nk_max,0.)
    call hbook1(107,'Photon thres',100,brem_min,brem_max,0.)
    call hbook1(113,'Jpsi CM theta ',100,0.,180.,0.)
    call hbook1(114,'Jpsi CM phi ',100,-180.,180.,0.)
    call hbook1(117,'Jpsi Lab theta ',100,0.,20.,0.)
    call hbook1(118,'Jpsi Lab phi ',100,-180.,180.,0.)
    call hbook1(121,'Muon1 Lab theta ',100,0.,180.,0.)
    call hbook1(122,'Muon1 Lab phi ',100,-180.,180.,0.)
    call hbook1(124,'Muon2 Lab theta ',100,0.,180.,0.)
    call hbook1(125,'Muon2 Lab phi ',100,-180.,180.,0.)
    call hbook2(301,'Lab P vs Lab theta',100,0.,180.,100,0.,180.0,30)
    call hbook1(200,'Random',100,0.,1.,0.)

C          get random deviates for nu and k

```

```

exp_int = -norm_exp/alpha*
>      (exp(-alpha*nk_max) - exp(-alpha*k_cutoff))
flat_int = norm_flat*(k_cutoff-nk_min)
x_cutoff = flat_int/(flat_int + exp_int)
finished = .false.
count = 0
nb_attempts=0
mj0 = mj
mjlow=mj0-mj_width*15
mjhi =mj0+mj_width*15
p=0
q=0
m=0
do while(.not.finished)
  nb_attempts=nb_attempts+1
C   do i =1,nb_events
C   if(mod(i,N).eq.N-1) write(6,*)'Processing event number: ',i+1
  if(mono_E) then
    nu = brem_max
    nk = 0.
    theta = 0.
    phi = 0.
  else
    brem_dev_range = log(brem_max/brem_min)
    random = rlu(irlu)
    brem_dev      = brem_dev_range*random+ log(brem_min)
    nu            = exp(brem_dev)
    ran_k = rlu(irlu)
    do ink=1,501
      if(x(ink).gt.ran_k) then
        lim=ink-1
        goto 10
      endif
    enddo
10  continue
    slope=(y(lim+1)-y(lim))/(x(lim+1)-x(lim))
    nk=y(lim)+slope*(ran_k-x(lim))
    theta = acos(2.0*rlu(irlu)-1.0)
    phi   = 2*pi*rndm(4)-pi
  endif
CX  if(ran_k.le.x_cutoff) then
CX  Nk = (exp_int+flat_int)/norm_flat*ran_k
CX  else
CX  Nk_dev_range= exp(-alpha*k_cutoff) - exp(-alpha*Nk_max)
CX  Nk_dev      = Nk_dev_range*rlu(irlu) + exp(-alpha*Nk_max)
CX  Nk          = -log(Nk_dev)/alpha
CX  endif

C Create j/psi's

Pg(1)=0.0
Pg(2)=0.0
Pg(3)=nu
Pg(4)=nu
Ep  = sqrt(Nk**2 + Mp**2) - (Nk**2)/(2*Mp) ! off-shell proton
s   = Ep*Ep-Nk*Nk +2.0*nu*Ep - 2.0*nu*Nk*cos(theta)

C Lorentz distribution for the mass
CALL FUNLXP(breit_wigner,XX,mjlow,mjhi)
CALL FUNLUX(XX,XRAN,1)
mj=XRAN
sth  = (Mj+Mp)**2

```

```

if(s.gt.sth) then
  keep = .true.
  if(weight)then
    crosssection = ballamfit(nu)
    rand = rlu(irlu)
    if(rand.ge.crosssection)then
      keep = .false.
    endif
  endif
endif
if(keep)then
  m=m+1
  if(t_dep.eq.0)then
    open(22,file='omegaevents0.dat',iostat=iocode,status='old')
    write(22,*)'Number of Omega Events: Uniform distribution:',m
    close(22)
  elseif(t_dep.eq.1)then
    open(22,file='omegaevents1.dat',iostat=iocode,status='old')
    write(22,*)'Number of Omega Events: Exp distribution:',m
    close(22)
  elseif(t_dep.eq.2)then
    open(22,file='omegaevents2.dat',iostat=iocode,status='old')
    write(22,*)'Number of Omega Events: OPE distribution:',m
    close(22)
  endif
C Nucleon momentum in lab coordinate system
  Pp(1) = Nk*sin(theta)*cos(phi)
  Pp(2) = Nk*sin(theta)*sin(phi)
  Pp(3) = Nk*cos(theta)
  Pp(4) = Ep
C Calculate photon energy in off-shell proton's rest frame
  beta(1) = (Pp(1))/(Ep)           !Beta is the vel of proton in LAB
  beta(2) = (Pp(2))/(Ep)
  beta(3) = (Pp(3))/(Ep)
  betasq = beta(1)**2+beta(2)**2+beta(3)**2
  beta(4) = (Ep)/sqrt(Ep**2-(Pp(1)**2+Pp(2)**2+Pp(3)**2))
  dir(1) = beta(1)/sqrt(betasq)    ! Dir is dir of beta in LAB
  dir(2) = beta(2)/sqrt(betasq)
  dir(3) = beta(3)/sqrt(betasq)
  call gloren(beta,Pp,Pprf)
  call gloren(beta,Pg,Pgrf)
* Calculate CM quantities
  beta(1) = (Pp(1)+pg(1))/(Ep+pg(4)) !Beta is the vel of CM in LAB
  beta(2) = (Pp(2)+pg(2))/(Ep+pg(4))
  beta(3) = (Pp(3)+pg(3))/(Ep+pg(4))
  betasq = beta(1)**2+beta(2)**2+beta(3)**2
  beta(4) = (Ep+Pg(4))/sqrt(s)
  dir(1) = beta(1)/sqrt(betasq)    ! Dir is dir of beta in LAB
  dir(2) = beta(2)/sqrt(betasq)
  dir(3) = beta(3)/sqrt(betasq)
  call gloren(beta,Pp,Ppcm)
  call gloren(beta,Pg,Pgcm)
* Calculate CM energies, momenta of j/psi and recoiling proton
  Eppcm = (s+Mp**2-Mj**2)/(2*sqrt(s)) ! recoiling proton cm energy
  Ejcm = sqrt(s)-Eppcm                ! j/psi's cm energy
  Pppcm = sqrt(Eppcm**2-Mp**2)
  Pjcm = Pppcm
  if(t_dep.eq.1) then              ! theta weighted by dsig/dt=exp(bt)
    pgcm_mag = sqrt(pgcm(1)**2+pgcm(2)**2+pgcm(3)**2)
    t_min = Mj**2 - 2.0*Pgcm(4)*Ejcm + 2.0*Pgcm_mag*Pjcm
    t_max = Mj**2 - 2.0*Pgcm(4)*Ejcm - 2.0*Pgcm_mag*Pjcm
    t_dev_range = exp(b*t_min) - exp(b*t_max)
    t_dev = t_dev_range+rlu(9) + exp(b*t_max)
    t = 1/b*log(t_dev)

```

```

      thjcm = acos((t-Mj**2+2*Pgcm(4)*Ejcm)/(2*Pgcm_mag*Pjcm))
elseif(t_dep.eq.2) then ! diffractive cross-section terms
  pgcm_mag = sqrt(pgcm(1)**2+pgcm(2)**2+pgcm(3)**2)
  t_min = abs(Mj**2 - 2.0*Pgcm(4)*Ejcm + 2.0*Pgcm_mag*Pjcm)
  t_max = abs(Mj**2 - 2.0*Pgcm(4)*Ejcm - 2.0*Pgcm_mag*Pjcm)
  if(t_max.gt.4.5)then
    q=q+1
    open(23,file='t_max.dat',iostat=iocode,status='old')
    write(23,*)'Value of s, t_min, t_max : ',s,t_min,t_max
    close(23)
    t_max = 4.5
    CALL FUNLXP(diff,YY,t_min,t_max)
    CALL FUNLUX(YY,YRAN,1)
    t=YRAN
  else
    CALL FUNLXP(diff,YY,t_min,t_max)
    CALL FUNLUX(YY,YRAN,1)
    t=YRAN
  endif
elseif(t_dep.eq.0)then
  thjcm = acos(2.0*rlu(irlu)-1) ! theta uniform in cos
  t = Mj**2-2.0*Pgcm(4)*Ejcm+2.0*Pgcm_mag*Pjcm*cos(thjcm)
endif
  phjcm = 2*pi*rlu(irlu)-pi ! phi uniform from -pi to pi
C J/psi momentum in lab coordinate system
  Pjcm_v(1) = Pjcm*sin(thjcm)*cos(phjcm)
  Pjcm_v(2) = Pjcm*sin(thjcm)*sin(phjcm)
  Pjcm_v(3) = Pjcm*cos(thjcm)
  Pjcm_v(4) = Ejcm
  do j = 1,3 ! beta to go from CM to lab
    beta(j)=-beta(j)
  enddo
  call gloren(beta,Pjcm_v,Pjlab_v)
  Pjlab = sqrt(Pjlab_v(1)**2+Pjlab_v(2)**2+Pjlab_v(3)**2)
  Ejlab = Pjlab_v(4)
  thjlab = acos(Pjlab_v(3)/Pjlab)
  if(Pjlab_v(1).lt.0.0) then
    if(Pjlab_v(2).gt.0.0) then
      phjlab = atan(Pjlab_v(2)/Pjlab_v(1))+pi
    else
      phjlab = atan(Pjlab_v(2)/Pjlab_v(1))-pi
    endif
  else
    phjlab = atan(Pjlab_v(2)/Pjlab_v(1))
  endif
C Decay j/psi into 2 muons
C
  call decay(pjlab_v,pcm,decay_ang_dep)
C
  pmul = sqrt(pcm(1,1)**2+pcm(2,1)**2+pcm(3,1)**2)
  thmul= acos(pcm(3,1)/pmul)
  if(pcm(2,1).lt.0.0) then
    if(pcm(1,1).gt.0.0) then
      phmul = atan(pcm(1,1)/pcm(2,1))+pi
    else
      phmul = atan(pcm(1,1)/pcm(2,1))-pi
    endif
  else
    phmul = atan(pcm(1,1)/pcm(2,1))
  endif
C Spectrometer angles
  phmul_s = asin(sin(thmul)*sin(phmul))
  thmul_s = acos(cos(thmul)/cos(phmul_s))

```

```

pmu2 = sqrt(pcm(1,2)**2+pcm(2,2)**2+pcm(3,2)**2)
thmu2= acos(pcm(3,2)/pmu2)
if(pcm(2,2).lt.0.0) then
  if(pcm(1,2).gt.0.0) then
    phmu2 = atan(pcm(1,2)/pcm(2,2))+pi
  else
    phmu2 = atan(pcm(1,2)/pcm(2,2))-pi
  endif
else
  phmu2 = atan(pcm(1,2)/pcm(2,2))
endif
C Spectrometer angles
  phmu2_s = asin(sin(thmu2)*sin(phmu2))
  thmu2_s = acos(cos(thmu2)/cos(phmu2_s))
C
C          Fill ntuple
> if(spect_cuts) call spectrom(pmu1,thmu1_s,phmu1_s,
  pmu2,thmu2_s,phmu2_s,record_ntuple)
if(record_ntuple) then
  angs(1) = nu
  angs(2) = Nk
  angs(3) = theta
  angs(4) = phi
  angs(5) = s
  angs(6) = Pjcm
  angs(7) = Ejcm
  angs(8) = thjcm*raddeg
  angs(9) = Phjcm*raddeg
  angs(10) = Pjlab
  angs(11) = Ejlab
  angs(12) = thjlab*raddeg
  angs(13) = Phjlab*raddeg
  angs(14) = z
  angs(15) = t
  angs(16) = t-t_min

  angs(20) = pmu1
  angs(21) = thmu1*raddeg
  angs(22) = phmu1*raddeg
  angs(23) = pmu2
  angs(24) = thmu2*raddeg
  angs(25) = phmu2*raddeg
  angs(26) = Pgrf(4)
  angs(27) = mj
  angs(28) = phmu1_s*raddeg
  angs(29) = thmu1_s*raddeg
  angs(30) = phmu2_s*raddeg
  angs(31) = thmu2_s*raddeg
  angs(32) = crosssection
C
  call hfn(9,angs)
  do j = 1,nb_var
    angs(j) = 0.0
  enddo
  count = count + 1
  if(count.ge.nb_events) finished = .true.
  if(mod(count,N).eq.N-1) then
    write(6,*)'Processing event number: ',count+1
  endif
endif
C
C          Fill histograms

```

```

C
      if(nb_attempts.le.1000000) then
        call hfill(105,s,0.,1.)
        call hfill(106,nk,0.,1.)
        call hfill(107,nu,0.,1.)
        call hfill(108,theta*raddeg,0.,1.)
        call hfill(110,pgrf(4),0.,1.)
        call hfill(111,Ejcm,0.,1.)
        call hfill(112,Pjcm,0.,1.)
        call hfill(113,thjcm*raddeg,0.,1.)
        call hfill(114,phjcm*raddeg,0.,1.)
        call hfill(115,Ejlab,0.,1.)
        call hfill(116,Pjlab,0.,1.)
        call hfill(117,thjlab*raddeg,0.,1.)
        call hfill(118,phjlab*raddeg,0.,1.)
        call hfill(120,pmul,0.,1.)
        call hfill(121,thmul*raddeg,0.,1.)
        call hfill(122,phmul*raddeg,0.,1.)
        call hfill(123,pmu2,0.,1.)
        call hfill(124,thmu2*raddeg,0.,1.)
        call hfill(125,phmu2*raddeg,0.,1.)
        call hfill(300,thmul*raddeg,pmul,1.)
        call hfill(301,thmul*raddeg,thmu2*raddeg,1.)
      endif
    endif
  endif
  if(nb_attempts.le.1000000) then
    call hfill(100,nu,0.,1.)
    call hfill(101,Nk,0.,1.)
    call hfill(102,theta*raddeg,0.,1.)
    call hfill(103,phi*raddeg,0.,1.)
    call hfill(104,s,0.,1.)

    call hfill(200,random,0.,1.)
  endif
enddo
write(6,*)'Number of times t > 4.0: ',p
write(6,*)'Number of times t_max > 4.0: ',q
write(6,*) 'The number of attempts is: ',nb_attempts
close(21)
call hrout(0,icycle,' ')
call hrend('jpsi')

C      do i=100,125
C        if(i.ne.109.and.i.ne.119) then
C          call hrput(i,filename,'n')
C        endif
C      enddo
c      call hrput(200,filename,'n')
c      call hrput(300,filename,'n')
c      call hrput(301,filename,'n')
end

C
C*****
      subroutine decay(jlab,gkin,ang_dep)
C
C          Hardwired for j/psi as parent particle
C          I should generate the mass from a Lorentz distribution
C          if the lifetime is less than 10^-15 sec
C
      integer irlu
      real*4  jlab(4)           ! Lab 4 momentum of parent particle
      real*4  jlab_mag         ! Lab 3 momentum squared

```



```

real*4 gkin(4,2)          ! Lab 4 momentum of decay particles
real*4 pcm(4,2)
real*4 beta(4)
real*4 dir(3)            ! direction of parent in Lab coordinate
real*4 costh,sinth,cosph,sinph
real*4 xm(2)
real*4 mj,pi,raddeg,mj_width,mj0
real*4 mmu/0.105659/
real  rlu
integer ang_dep          ! 0: isotropic in decay angle
                        ! 1: weighted by 1+cos(th_cm)**2

logical rotate

C
common/const/pi,raddeg,mj,mj0,mj_width
C
C      2 body decay
C
xm(1)=mmu
xm(2)=mmu

C
call deca2(mj,xm(1),xm(2),pcm,ang_dep)
C      boost into LAB along parent vector followed by rotation back into
C      correct coordinate system
C
jlab_mag = sqrt(jlab(1)**2+jlab(2)**2+jlab(3)**2)
do i = 1,3
  dir(i) = jlab(i)/jlab_mag
enddo
beta(1) = 0.0
beta(2) = 0.0
beta(3) = -jlab_mag/jlab(4)
beta(4) = jlab(4)/mj
call gfang(dir,costh,sinth,cosph,sinph,rotate)
C
do i = 1,2
  if(jlab_mag.le.0.0) then
    do j = 1,3
      gkin(j,i)=pcm(j,i)
    enddo
  else
    call gloren(beta,pcm(1,i),gkin(1,i))
  endif
endif
CX remove
rotate=.false.
CX
if(rotate) call gdrot(gkin(1,i),costh,sinth,cosph,sinph)
gkin(4,i)=sqrt(gkin(1,i)**2+gkin(2,i)**2+gkin(3,i)**2+xm(i)**2)
enddo
C
return
end

C
C*****
subroutine deca2(xm0,xm1,xm2,pcm,ang_dist)
C
implicit none
C
integer irlu
integer ang_dist      ! 0: isotropic in decay angle; 1: 1+cos^2(theta)
real*4 xm0            ! mass of parent particle
real*4 xm1,xm2        ! masses of two body decay products
real*4 pcm(4,2)      ! momenta of decay products

```

```

real*4 costh,sinth
real*4 phi
real*4 E1,P1
real*4 twopi/6.283185307/
real*4 raddeg/57.29578/
C
C
integer nb_var
parameter (nb_var=32)
real*4 angs(nb_var)
common/ntup/angs
C
external rndm
real*4 rndm
real rlu
C
C      Generate first decay product in CMS
C
E1=(xm0*xm0+xm1*xm1-xm2*xm2)/(2*xm0)
P1=sqrt(abs((E1-xm1)*(E1+xm1)))
C
C      Generate angular distribution
C
if(ang_dist.eq.0) then
  costh=2.*rlu(irlu)-1.
else
30  costh=2.*rlu(irlu)-1.
  if(2*rlu(irlu).ge.(1+(costh)**2)) goto 30
endif
if(abs(costh).ge.1.0) then
  costh=sign(1.0,costh)
  sinth=0.
else
  sinth=sqrt((1.-costh)*(1.+costh))
endif
phi=twopi*rlu(irlu)
C
angs(17) = p1
angs(18) = acos(costh)*raddeg
angs(19) = phi*raddeg
C
C
C      Polar co-ordinates to momentum components
C
pcm(1,1)=P1*sinth*cos(phi)
pcm(2,1)=P1*sinth*sin(phi)
pcm(3,1)=P1*costh
pcm(4,1)=E1
C
C      Generate second decay product
C
pcm(1,2)=-pcm(1,1)
pcm(2,2)=-pcm(2,1)
pcm(3,2)=-pcm(3,1)
pcm(4,2)=sqrt(pcm(1,2)**2+pcm(2,2)**2+pcm(3,2)**2+xm2*xm2)
C
return
end
C*****
subroutine spectrom(p1,th1,ph1,p2,th2,ph2,record)
C
C      See if muons make it into the spectrometers
C

```

```

C
  real*4 p1,th1,ph1,p2,th2,ph2
  logical record
  real*4 ph1_s,ph2_s
  real*4 sos_p0,sos_p_range,sos_th0,sos_th_range,sos_ph0,
>   sos_ph_range, hms_p0,hms_p_range,hms_th0,hms_th_range,
>   hms_ph0,hms_ph_range
  common/spect_cuts/sos_p0,sos_p_range,sos_th0,sos_th_range,
>   sos_ph0,sos_ph_range,hms_p0,hms_p_range,
>   hms_th0,hms_th_range,hms_ph0,hms_ph_range

C
  record=.false.
C
  ph1_s=atan(tan(ph1)*sin(th1))
C
  ph2_s=atan(tan(ph2)*sin(th2))
  if(ph1.ge.sos_ph0-sos_ph_range.and.
>   ph1.le.sos_ph0+sos_ph_range) then
    if(ph2.ge.hms_ph0-hms_ph_range.and.
>   ph2.le.hms_ph0+hms_ph_range) then
      if(th1.ge.sos_th0-sos_th_range.and.
>   th1.le.sos_th0+sos_th_range) then
        if(th2.ge.hms_th0-hms_th_range.and.
>   th2.le.hms_th0+hms_th_range) then
          if(p1.ge.sos_p0*(1.0-sos_p_range).and.
>   p1.le.sos_p0*(1.0+sos_p_range)) then
            if(p2.ge.hms_p0*(1.0-hms_p_range).and.
>   p2.le.hms_p0*(1.0+hms_p_range)) then
              record=.true.
            endif
          endif
        endif
      endif
    endif
  endif
  return
end

C
BREIT-WIGNER MASS DISTRIBUTION FUNCTION

real*4 function Breit_Wigner(x)
real*4 pi,raddeg,mj,mj_width,mj0
common/const/pi,raddeg,mj,mj0,mj_width

Breit_Wigner=
> 1./(mj0*pi*mj_width*(1+((x**2-mj0**2)/(mj0*mj_width))**2)))
return
end

C
FUNCTION FOR ONE PION EXCHANGE AND DIFFRACTIVE CROSS-SECTION

real*4 function diff(t)
real*4 pi,raddeg,mj,mj_width,mj0,s
common/const/pi,raddeg,mj,mj0,mj_width
common s

diff = (0.215e4*t*(.25*(.880-s)*(1.49-s+t)-.25*(s**(1/2)-.938)**2*
>(s**(1/2)+.938)**2)**2*(0.472e-1*(4.34*t**2+5.28*t+2.63)*log(8.68
>*t**2+10.6*t+4.26)/(.410*t**2+.500*t+.154)-1)/((s-.880)**2*s*(t+
>.196e-1)**2*(s**(1/2)-.938)**2*(s**(1/2)+.938)**2*(1+2.40*t*(t+3.5
>2))*(.410*t**2+.500*t+.154)**2))+(62.61*exp(-6.7*t)*(1+(2.626/
>(s-0.879))))!differential cross-section OPE and diffractive terms
C (THIS DIFFERENTIAL CROSS-SECTION IS OBTAINED BY PLUGGING t=(-t) IN ORIGINAL CODE)
C
  continue
  return

```

```

end

C      FUNCTION FOR CROSS-SECTION FIT FOR BALLAM DATA

      real*4 function ballamfit(z)
      ballamfit =
      >.8442613249+(.1592945896*((z-2.8)/(.2831924835-.2360169021*z)))
C THIS FUNCTION IS TO BE USED ONLY WHEN spect_cuts IS ON
C BCOZ IT IS OVER THE RANGE brem_min to brem_max
      continue
      return
      end

C*****

      SUBROUTINE FUNLXP (FUNC,XFCUM,X2LOW,X2HIGH)
      F. JAMES, Sept, 1994
C
C      Prepares the user function FUNC for FUNLUX
C      Inspired by and mostly copied from FUNPRE and FUNRAN
C      except that
C      1. FUNLUX uses RANLUX underneath,
C      2. FUNLXP expands the first and last bins to cater for
C          functions with long tails on left and/or right,
C      3. FUNLXP calls FUNPCT to do the actual finding of percentiles.
C      4. both FUNLXP and FUNPCT use RADAPT for Gaussian integration.
C
      real*4 tftot, rsteps, x2low, x2high, xlow, xhigh
      integer*4 ifunc,ierr
      real*4 uncert, x2, x3, tftot1, tftot2, xrange
      EXTERNAL FUNC
      DIMENSION XFCUM(200)
      COMMON/FUNINT/TFTOT
      PARAMETER (RTEPS=0.0002)
      SAVE IFUNC
      DATA IFUNC/0/

      IFUNC = IFUNC + 1
C      FIND RANGE WHERE FUNCTION IS NON-ZERO.
      CALL FUNLZ(FUNC,X2LOW,X2HIGH,XLOW,XHIGH)
      XRRANGE = XHIGH-XLOW
      IF(XRRANGE .LE. 0.) THEN
      WRITE (6,'(A,2G15.5)') ' FUNLXP finds function range .LE.0',
+ XLOW,XHIGH
      GO TO 900
      ENDIF
      CALL RADAPT(FUNC,XLOW,XHIGH,1,RTEPS,0.,TFTOT ,UNCERT)
C      WRITE(6,1003) IFUNC,XLOW,XHIGH,TFTOT
C 1003 FORMAT(' FUNLXP: integral of USER FUNCTION',
+ I3,' from ',E12.5,' to ',E12.5,' is ',E14.6)
C
C      WRITE (6,'(A,A)') ' FUNLXP preparing ',
C      + 'first the whole range, then left tail, then right tail.'
      CALL FUNPCT(FUNC,IFUNC,XLOW,XHIGH,XFCUM,1,99,TFTOT,IERR)
      IF (IERR .GT. 0) GO TO 900
      X2 = XFCUM(3)
      CALL RADAPT(FUNC,XLOW,X2,1,RTEPS,0.,TFTOT1 ,UNCERT)
      CALL FUNPCT(FUNC,IFUNC,XLOW,X2 ,XFCUM,101,49,TFTOT1,IERR)
      IF (IERR .GT. 0) GO TO 900
      X3 = XFCUM(98)
      CALL RADAPT(FUNC,X3,XHIGH,1,RTEPS,0.,TFTOT2 ,UNCERT)

```

```

        CALL FUNPCT(FUNC,IFUNC,X3,XHIGH,XFCUM,151,49,TFTOT2,IERR)
        IF (IERR .GT. 0) GO TO 900
C       WRITE(6,1001) IFUNC,XLOW,XHIGH
C 1001 FORMAT(' FUNLXP has prepared USER FUNCTION',I3,
C       + ' between',G12.3,' and',G12.3,' for FUNLUX')
        RETURN
    900 CONTINUE
        WRITE (6,'(A)') ' Fatal error in FUNLXP. FUNLUX will not work.'
        END
C
        SUBROUTINE FUNPCT(FUNC,IFUNC,XLOW,XHIGH,XFCUM,NLO,NBINS,TFTOT,
+           IERR)
C       Array XFCUM is filled from NLO to NLO+NBINS, which makes
C       the number of values NBINS+1, or the number of bins NBINS
        EXTERNAL FUNC
        DIMENSION XFCUM(*)
        PARAMETER (RTEPS=0.005, NZ=10, MAXZ=20, NITMAX=6,PRECIS=1.E-6)
CC       DOUBLE PRECISION TPCTIL, TZ, TCUM, XINCR, DTABS,
CC       + TINCR, TZMAX, XBEST, DTBEST, DTPAR2
C
        IERR = 0
        IF (TFTOT .LE. 0.) GO TO 900
        TPCTIL = TFTOT/NBINS
        TZ = TPCTIL/NZ
        TZMAX = TZ * 2.
        XFCUM(NLO) = XLOW
        XFCUM(NLO+NBINS) = XHIGH
        X = XLOW
        F = FUNC(X)
        IF (F .LT. 0.) GO TO 900
C       Loop over percentile bins
        DO 600 IBIN = NLO, NLO+NBINS-2
            TCUM = 0.
            X1 = X
            F1 = F
            DXMAX = (XHIGH -X) / NZ
            FMIN = TZ/DXMAX
            FMINZ = FMIN
C       Loop over trapezoids within a supposed percentile
            DO 500 IZ= 1, MAXZ
                XINCR = TZ/MAX(F1,FMIN,FMINZ)
350 X = X1 + XINCR
                F = FUNC(X)
                IF (F .LT. 0.) GO TO 900
                TINCR = (X-X1) * 0.5 * (F+F1)
                IF (TINCR .LT. TZMAX) GO TO 370
                XINCR = XINCR * 0.5
                GO TO 350
370 CONTINUE
                TCUM = TCUM + TINCR
                IF (TCUM .GE. TPCTIL*0.99) GO TO 520
                FMINZ = TZ*F/ (TPCTIL-TCUM)
                F1 = F
                X1 = X
500 CONTINUE
                WRITE(6,'(A)') ' FUNLUX: WARNING. FUNPCT fails trapezoid.'
C       END OF TRAPEZOID LOOP
C       Adjust interval using Gaussian integration with
C       Newton corrections since F is the derivative
520 CONTINUE
            X1 = XFCUM(IBIN)
            XBEST = X
            DTBEST = TPCTIL

```

```

TPART = TPCTIL
C      Allow for maximum NITMAX more iterations on RADAPT
DO 550 IHOME= 1, NITMAX
535 XINCR = (TPCTIL-TPART) / MAX(F,FMIN)
X = XBEST + XINCR
X2 = X
IF (IHOME .GT. 1 .AND. X2 .EQ. XBEST) THEN
WRITE (6,'(A,G12.3)')
+ ' FUNLUX: WARNING from FUNPCT: insufficient precision at X=',X
GO TO 580
ENDIF
REFX = ABS(X)+PRECIS
CALL RADAPT(FUNC,X1,X2,1,RTEPS,0.,TPART2,UNCERT)
DTPAR2 = TPART2-TPCTIL
DTABS = ABS(DTPAR2)
IF(ABS(XINCR)/REFX .LT. PRECIS) GOTO 545
IF(DTABS .LT. DTBEST) GOTO 545
XINCR = XINCR * 0.5
GOTO 535
545 DTBEST = DTABS
XBEST = X
TPART = TPART2
F = FUNC(X)
IF(F .LT. 0.) GOTO 900
IF(DTABS .LT. RTEPS*TPCTIL) GOTO 580
550 CONTINUE
WRITE (6,'(A,I4)')
+ ' FUNLUX: WARNING from FUNPCT: cannot converge, bin',IBIN
C
580 CONTINUE
XINCR = (TPCTIL-TPART) / MAX(F,FMIN)
X = XBEST + XINCR
XFCUM(IBIN+1) = X
F = FUNC(X)
IF(F .LT. 0.) GOTO 900
600 CONTINUE
C      END OF LOOP OVER BINS
X1 = XFCUM(NLO+NBINS-1)
X2 = XHIGH
CALL RADAPT(FUNC,X1,X2,1,RTEPS,0.,TPART ,UNCERT)
ABERR = ABS(TPART-TPCTIL)/TFTOT
C      WRITE(6,1001) IFUNC,XLOW,XHIGH
C      IF(ABERR .GT. RTEPS) WRITE(6,1002) ABERR
RETURN
900 WRITE(6,1000) X,F
IERR = 1
RETURN
1000 FORMAT('/ FUNLUX fatal error in FUNPCT: function negative:/'
+ ', ' at X=',E15.6,', F=',E15.6/)
C 1001 FORMAT(' FUNPCT has prepared USER FUNCTION',I3,
C      + ' between',G12.3,' and',G12.3,' for FUNLUX.')
C 1002 FORMAT(' WARNING: Relative error in cumulative distribution',
C      + ' may be as big as',F10.7)
END
SUBROUTINE FUNLUX(ARRAY,XRAN,LEN)
C      Generation of LEN random numbers in any given distribution,
C      by 4-point interpolation in the inverse cumulative distr.
C      which was previously generated by FUNLXP
COMMON/FUNINT/XUNI
DIMENSION ARRAY(200)
DIMENSION XRAN(LEN)
C Bin width for main sequence, and its inverse
PARAMETER (GAP= 1./99., GAPINV=99.)

```

```

C Top of left tail, bottom of right tail (each tail replaces 2 bins)
  PARAMETER (TLEFT= 2./99.,BRIGHT=97./99.)
C Bin width for minor sequences (tails), and its inverse
  PARAMETER (GAPS=TLEFT/49., GAPINS=1./GAPS)
C
C The array ARRAY is assumed to have the following structure:
C   ARRAY(1-100) contains the 99 bins of the inverse cumulative
C               distribution of the entire function.
C   ARRAY(101-150) contains the 49-bin blowup of main bins
C               1 and 2 (left tail of distribution)
C   ARRAY(151-200) contains the 49-bin blowup of main bins
C               98 and 99 (right tail of distribution)
C
  CALL RANLUX(XRAN,LEN)

  DO 500 IBUF= 1, LEN
  X = XRAN(IBUF)
  J = INT( X *GAPINV) + 1
  IF (J .LT. 3) THEN
    J1 = INT( X *GAPINS)
    J = J1 + 101
    J = MAX(J,102)
    J = MIN(J,148)
    P = ( X -GAPS*(J1-1)) * GAPINS
    A = (P+1.0) * ARRAY(J+2) - (P-2.0)*ARRAY(J-1)
    B = (P-1.0) * ARRAY(J) - P * ARRAY(J+1)
    XRAN(IBUF) = A*P*(P-1.0)*0.16666667 + B*(P+1.0)*(P-2.0)*0.5
  ELSE IF (J .GT. 97) THEN
    J1 = INT((X-BRIGHT)*GAPINS)
    J = J1 + 151
    J = MAX(J,152)
    J = MIN(J,198)
    P = (X -BRIGHT -GAPS*(J1-1)) * GAPINS
    A = (P+1.0) * ARRAY(J+2) - (P-2.0)*ARRAY(J-1)
    B = (P-1.0) * ARRAY(J) - P * ARRAY(J+1)
    XRAN(IBUF) = A*P*(P-1.0)*0.16666667 + B*(P+1.0)*(P-2.0)*0.5
  ELSE
    J = MAX(J,2)
    J = MIN(J,98)
    P = ( X -GAP*(J-1)) * GAPINV
    A = (P+1.0) * ARRAY(J+2) - (P-2.0)*ARRAY(J-1)
    B = (P-1.0) * ARRAY(J) - P * ARRAY(J+1)
    XRAN(IBUF) = A*P*(P-1.0)*0.16666667 + B*(P+1.0)*(P-2.0)*0.5
  ENDIF
500 CONTINUE
  XUNI = X
  RETURN
  END
  SUBROUTINE FUNLZ(FUNC,X2LOW,X2HIGH,XLOW,XHIGH)
  C   FIND RANGE WHERE FUNC IS NON-ZERO.
  C   WRITTEN 1980, F. JAMES
  C   MODIFIED, NOV. 1985, TO FIX BUG AND GENERALIZE
  C   TO FIND SIMPLY-CONNECTED NON-ZERO REGION (XLOW,XHIGH)
  C   ANYWHERE WITHIN THE GIVEN REGION (X2LOW,H2HIGH).
  C   WHERE 'ANYWHERE' MEANS EITHER AT THE LOWER OR UPPER
  C   EDGE OF THE GIVEN REGION, OR, IF IN THE MIDDLE,
  C   COVERING AT LEAST 1% OF THE GIVEN REGION.
  C   OTHERWISE IT IS NOT GUARANTEED TO FIND THE NON-ZERO REGION.
  C   IF FUNCTION EVERYWHERE ZERO, FUNLZ SETS XLOW=XHIGH=0.
  EXTERNAL FUNC
  XLOW = X2LOW
  XHIGH = X2HIGH
  C   FIND OUT IF FUNCTION IS ZERO AT ONE END OR BOTH

```

```

        XMID = XLOW
        IF (FUNC(XLOW) .GT. 0.) GO TO 120
        XMID = XHIGH
        IF (FUNC(XHIGH) .GT. 0.) GO TO 50
C         FUNCTION IS ZERO AT BOTH ENDS,
C         LOOK FOR PLACE WHERE IT IS NON-ZERO.
        DO 30 LOGN= 1, 7
        NSLICE = 2**LOGN
        DO 20 I= 1, NSLICE, 2
        XMID = XLOW + I * (XHIGH-XLOW) / NSLICE
        IF (FUNC(XMID) .GT. 0.) GO TO 50
20      CONTINUE
30      CONTINUE
C         FALLING THROUGH LOOP MEANS CANNOT FIND NON-ZERO VALUE
        WRITE(6,554)
        WRITE(6,555) XLOW, XHIGH
        XLOW = 0.
        XHIGH = 0.
        GO TO 220
C
50      CONTINUE
C         DELETE 'LEADING' ZERO RANGE
        XH = XMID
        XL = XLOW
        DO 70 K= 1, 20
        XNEW = 0.5*(XH+XL)
        IF (FUNC(XNEW) .EQ. 0.) GO TO 68
        XH = XNEW
        GO TO 70
68      XL = XNEW
70      CONTINUE
        XLOW = XL
        WRITE(6,555) X2LOW,XLOW
120     CONTINUE
        IF (FUNC(XHIGH) .GT. 0.) GO TO 220
C         DELETE 'TRAILING' RANGE OF ZEROES
        XL = XMID
        XH = XHIGH
        DO 170 K= 1, 20
        XNEW = 0.5*(XH+XL)
        IF (FUNC(XNEW) .EQ. 0.) GO TO 168
        XL = XNEW
        GO TO 170
168     XH = XNEW
170     CONTINUE
        XHIGH = XH
        WRITE(6,555) XHIGH, X2HIGH
C
220     CONTINUE
        RETURN
554     FORMAT('CANNOT FIND NON-ZERO FUNCTION VALUE')
555     FORMAT(' FUNCTION IS ZERO FROM X=',E12.5,' TO ',E12.5)
        END

```